We have 3 lectures left:

Feb. 9th – lecture 11 – Today's, and Feb. 14th
Feb. 16th – lecture 12 – and Feb. 21st
Feb. 23th – lecture 13 – and Feb. 28th

Mar. 2nd – exam at CAMK at room 18/19
Mar. 9th – overview of exam, signing cards

You can still upload your HW#6 and hands-on results
Up to the Feb. 19th (Copernicus birthday).

The theory of different emission processes across astrophysical objects:

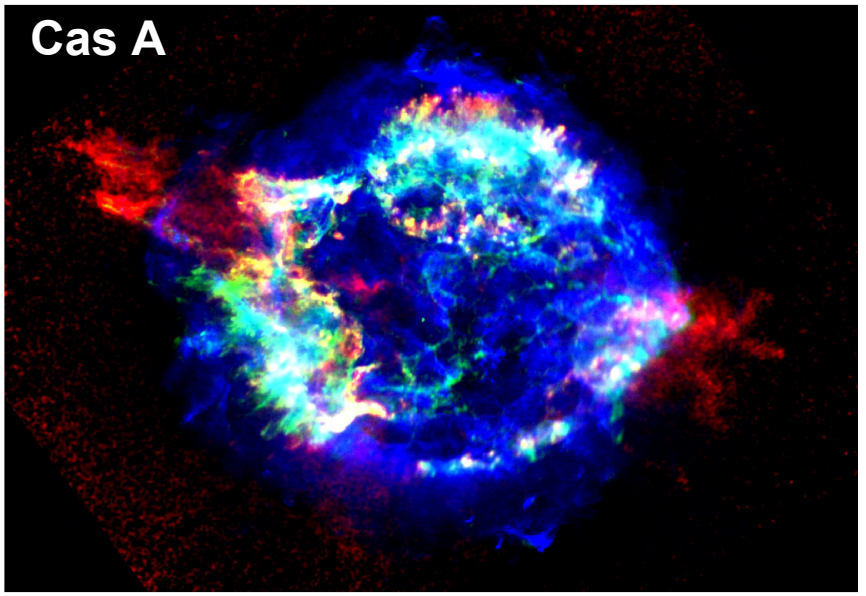

- Solar system objects
- Nuclear Burning Stars
- White Dwarfs
- Cataclysmic Variables
- Classical Novae
- Pulsars and Isolated Neutron Stars
- Accreting Neutrons Stars and Black Hole binaries
- Supernova Remnants
- Interstellar Medium
- Galactic Center

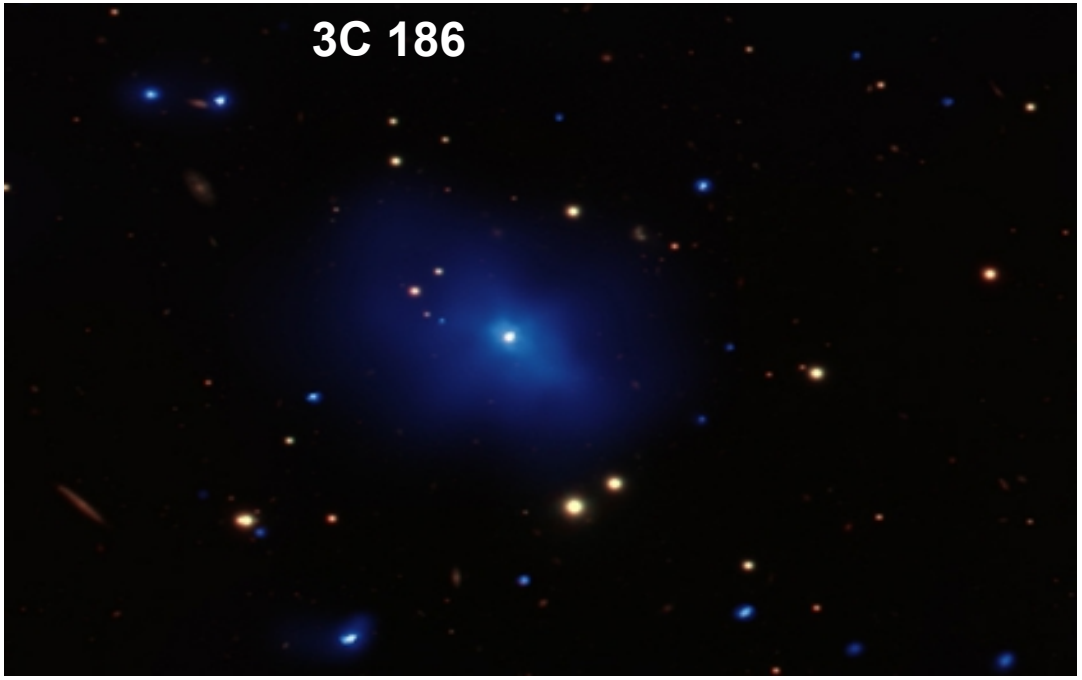

- Nearby Galaxies
- Active Galactic Nuclei
- Clusters of Galaxies
- Gamma- Ray Bursts
- Cosmic X-ray Background

Lecture 11th : Towards the Galactic Center

SNRs, ISM, Galactic Center....

SNRs – most photogenic X-ray sources:

Crab Nebula – first X-ray source associated with radio/optical object,

Cassiopeia A – first X-ray source with strong line emission,

First extended X-ray sources to be imaged.

Crab Nebula
Chandra

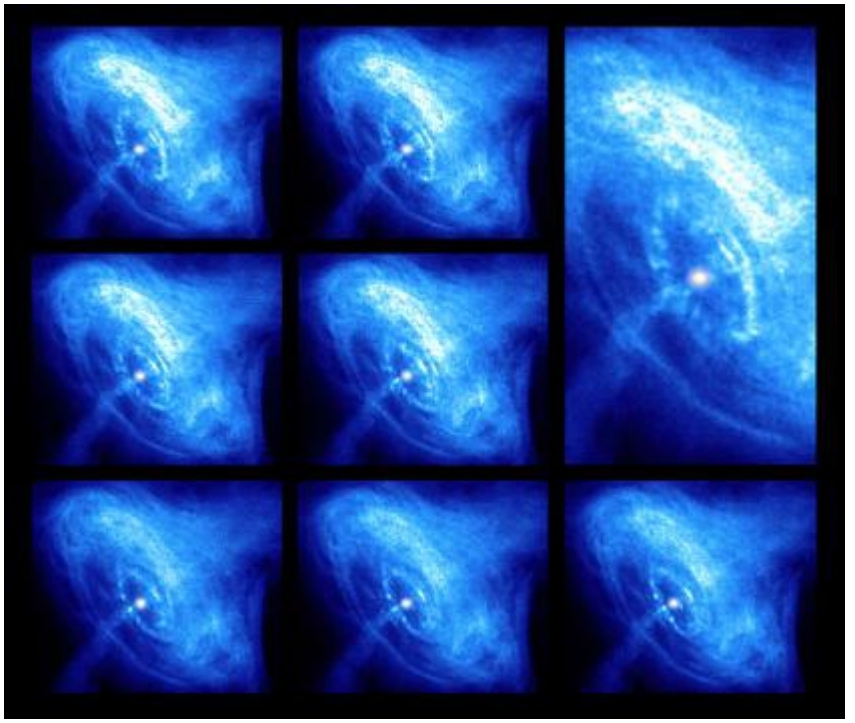

SNRs:

Ejecta heated by a reverse shock:

- low density , shock-heated plasma, non-equilibrium ionization (NEI) is less ionized than one in collisional ionization equilibrium (CIE) at the same electron temperature.

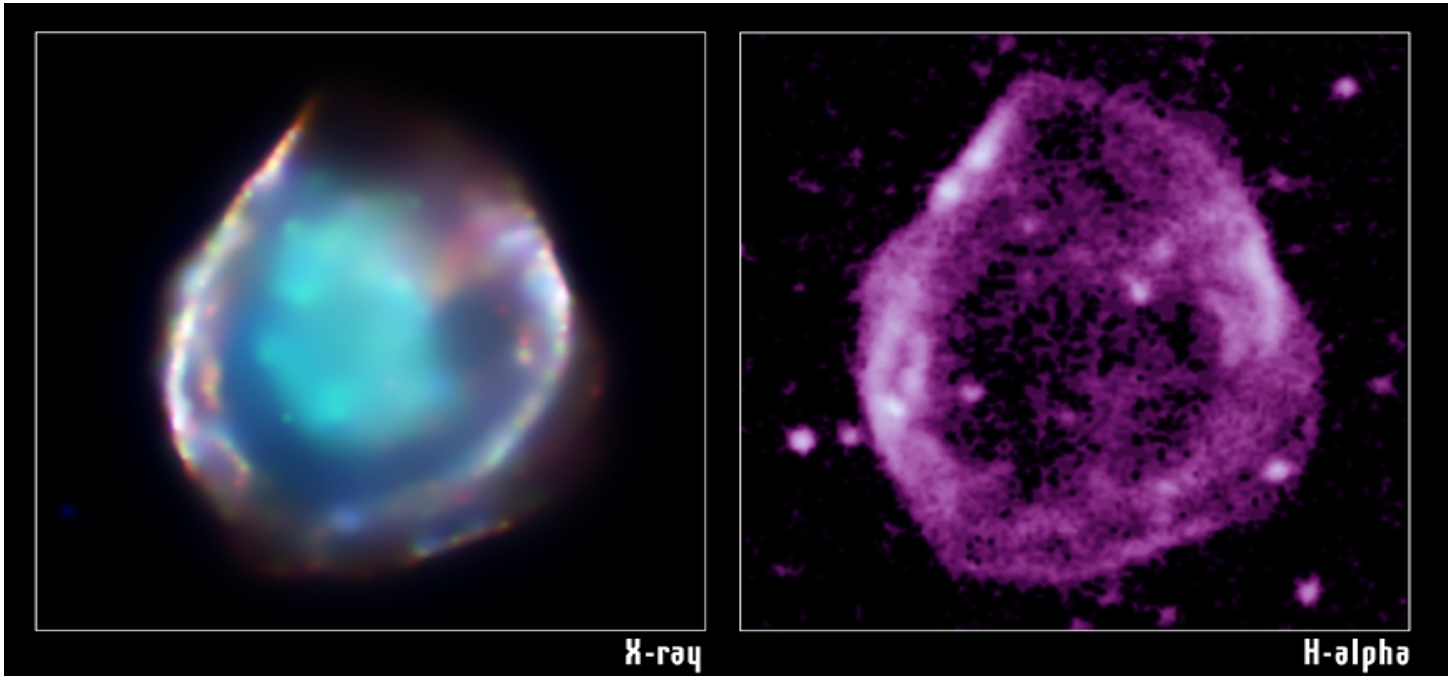

LMC remnant DEM L71 has an outer forward shock structure and an interior filled with Si and Fe rich material
0.3-0.7 keV red; 0.7-1 keV green ; 1.1-4.2 keV blue.

SNRs Type Ia:

They are only two confirmed Galactic Type Ia remnants:

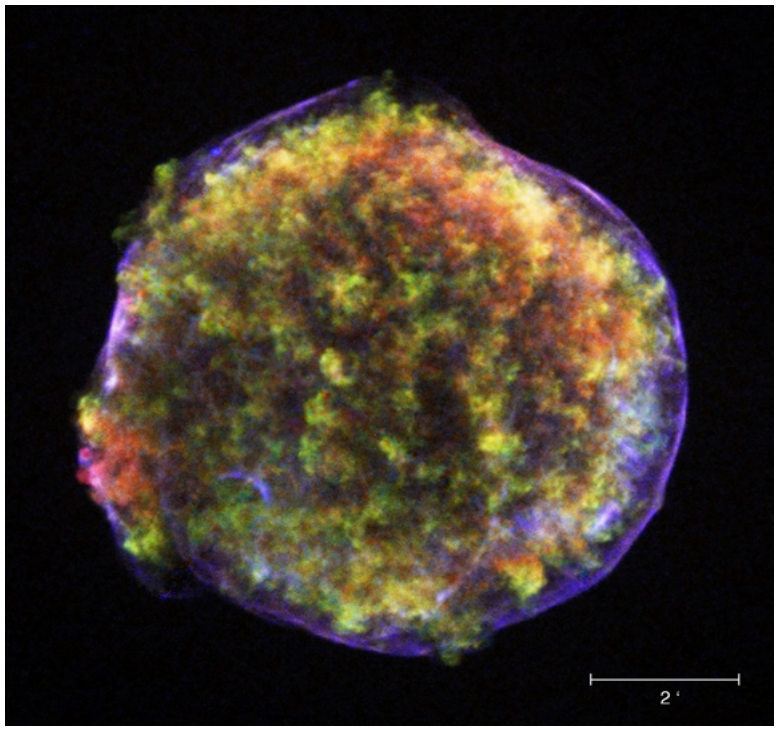

Tycho – Chandra

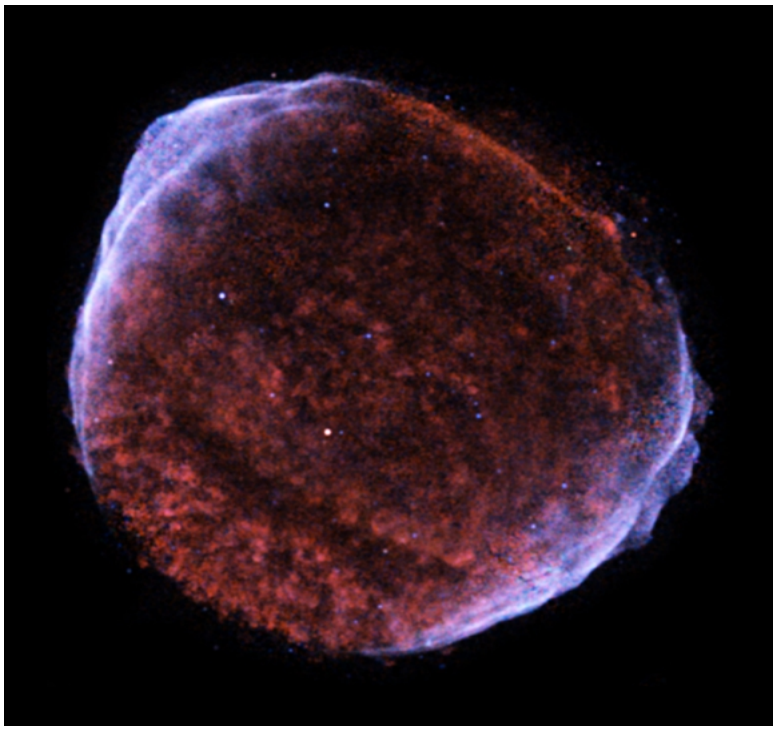

SN 1006 – ACIS

0.95-1.26 red
1.63-2.26 green
4.1-6.1 blue

Hard outer rim, angular diameter 8 arcmin, physical size 5.8 at D=2.5 kpc

0.50-0.91 red
0.91-1.34 cyan
1.34-3.0 blue

Plum like structure – 30 arcmin across, physical diameter of 18 pc at D=2.1 kpc

Core Collapse Remnants:

Variety of ejecta structures, from highly stratified to nearly chaotic.

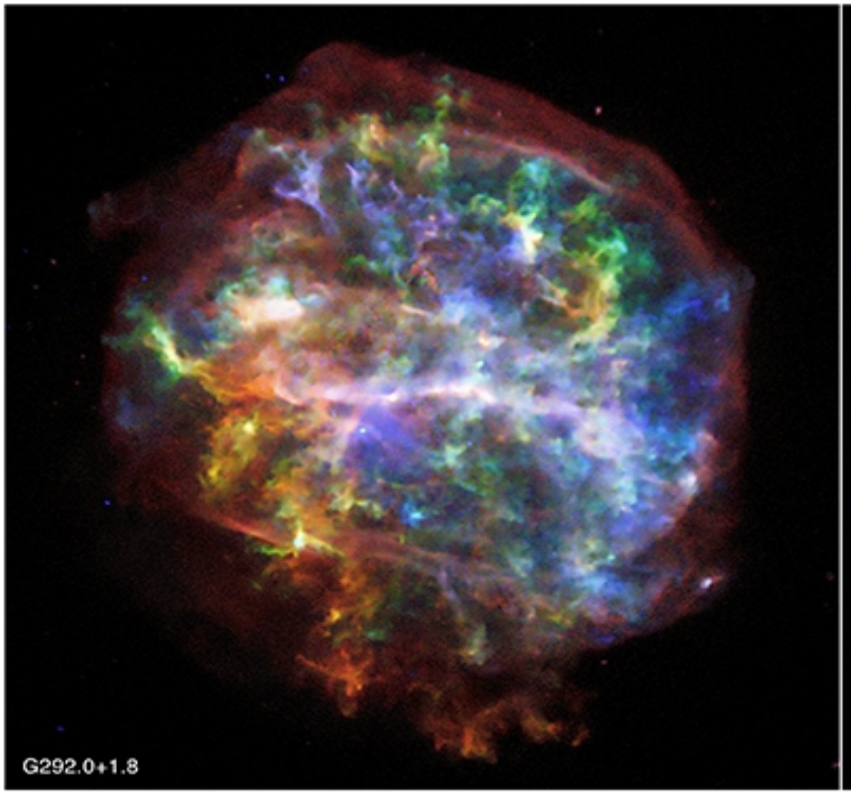

About 1600 yrs SNR,
Oxygen rich optical spectrum,
X-ray pulsar near the center.

No compact source has been found, but presence of high-density material surrounding the object. Total ejected mass about 1.4 M_Sun – Type Ia origin not excluded.

SNRs – shock structures:

First clear location of Cas A's forward and reverse shocks.

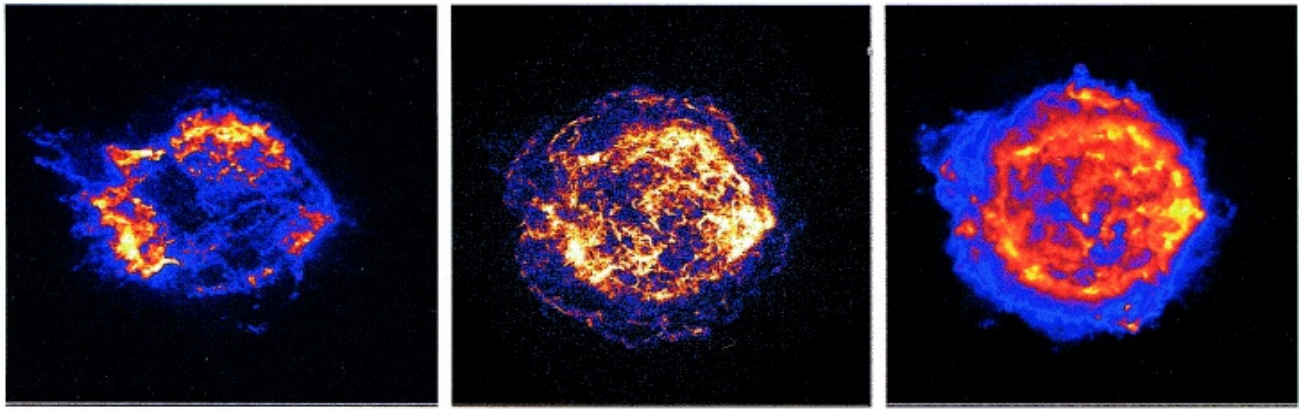

Chandra + Radio Gotthelf + 2001
3:2 diameter ratio of the forward and reverse shock.

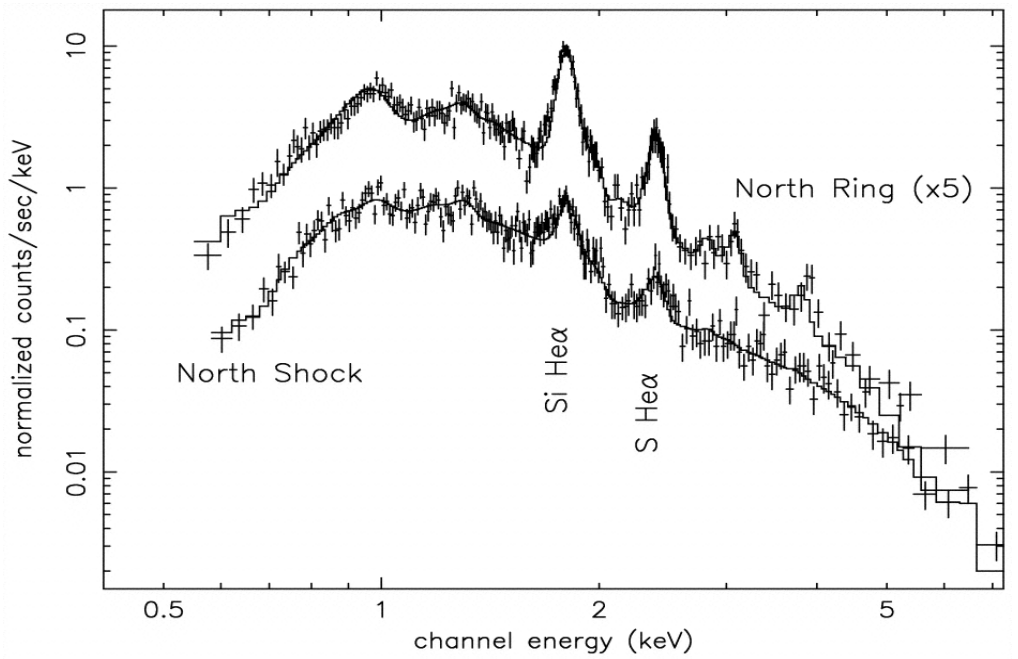

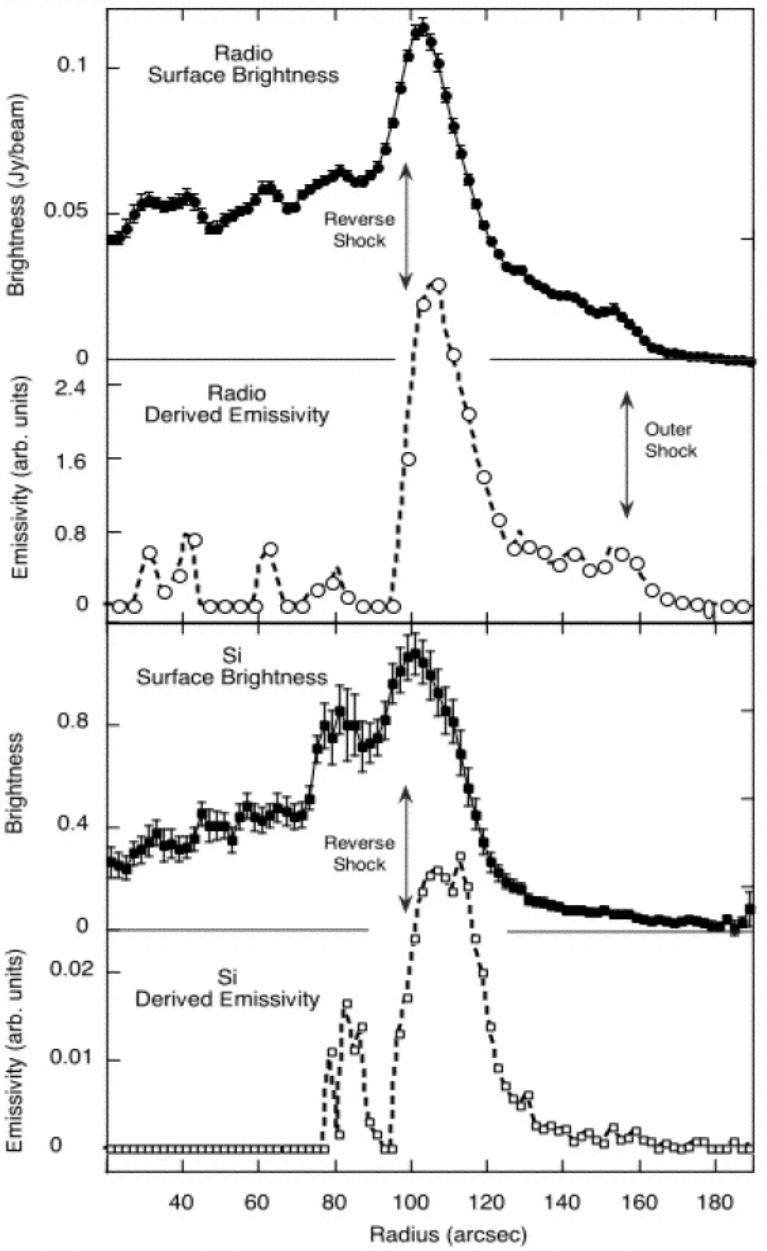

SNRs and their X-ray spectra:

ASCA and XMM spectra of W49B show ratios of abundances to solar of 5-6 for Si, S, Ca, Ar, Mg, and Fe.

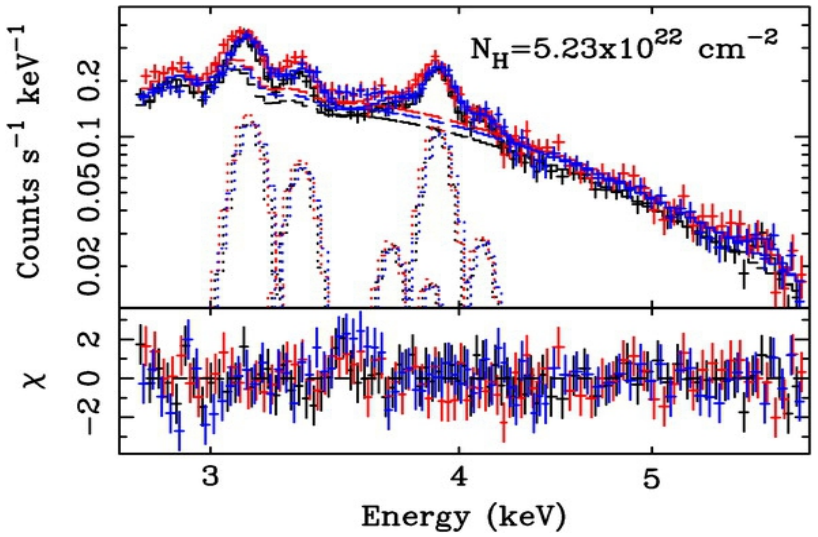

Kawasaki + 2005

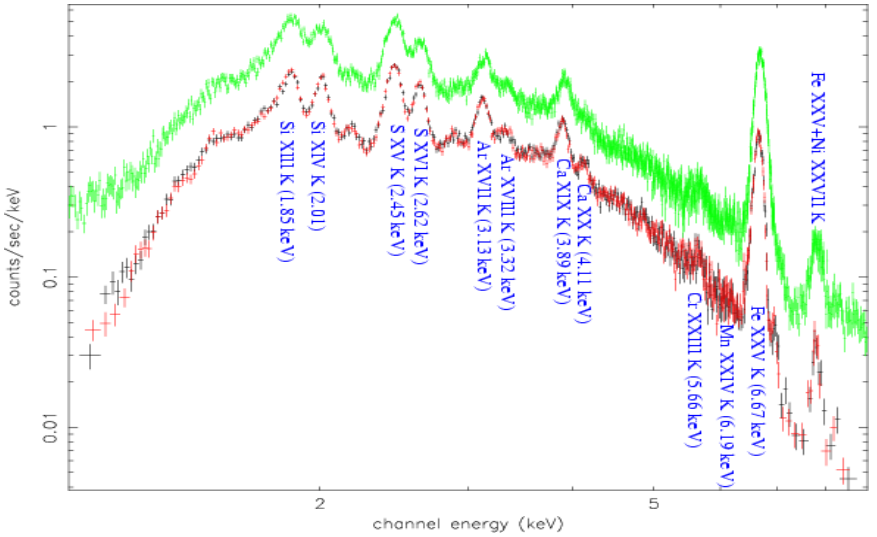

Miceli + 2006

Spectra are most commonly fitted with thermal bremsstrahlung for continuum and Gaussian emission lines for non equilibrium plasma.

SNRs:

Core collapse SNe have high ratio of oxygen and iron compared with cosmic abundances

Type Ia deflagration/detection have the opposite.

Oxygen abundance is difficult to determine as the oxygen line strength correlates with the column density.

Puppis A with Einstein

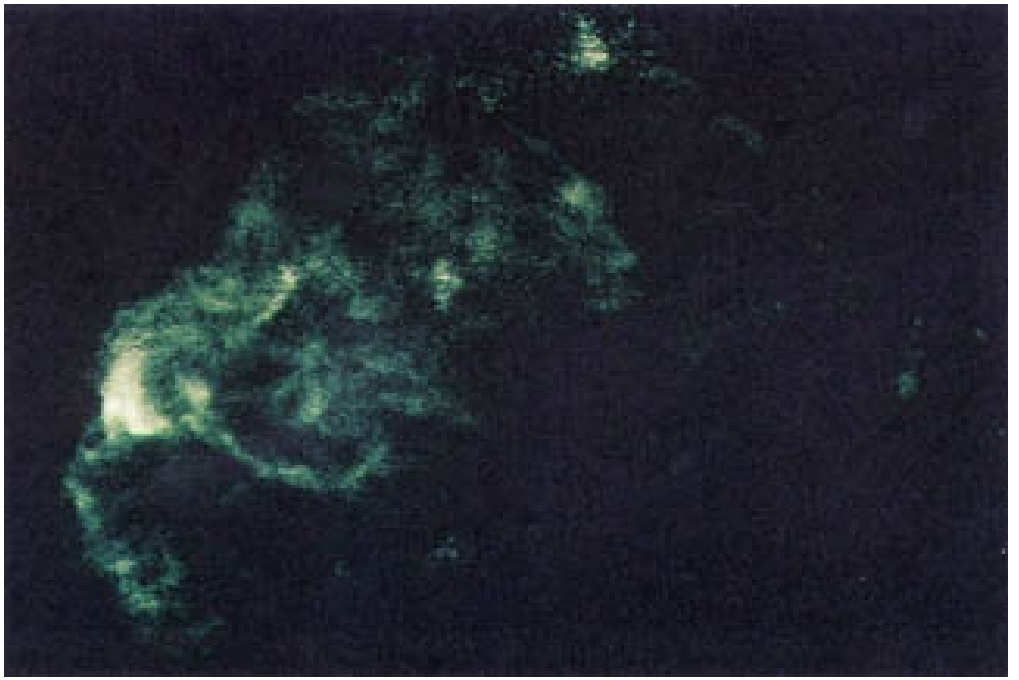

SNRs:

Rakowski + 2003, DEN L71, regions of spectral extraction:

Chandra

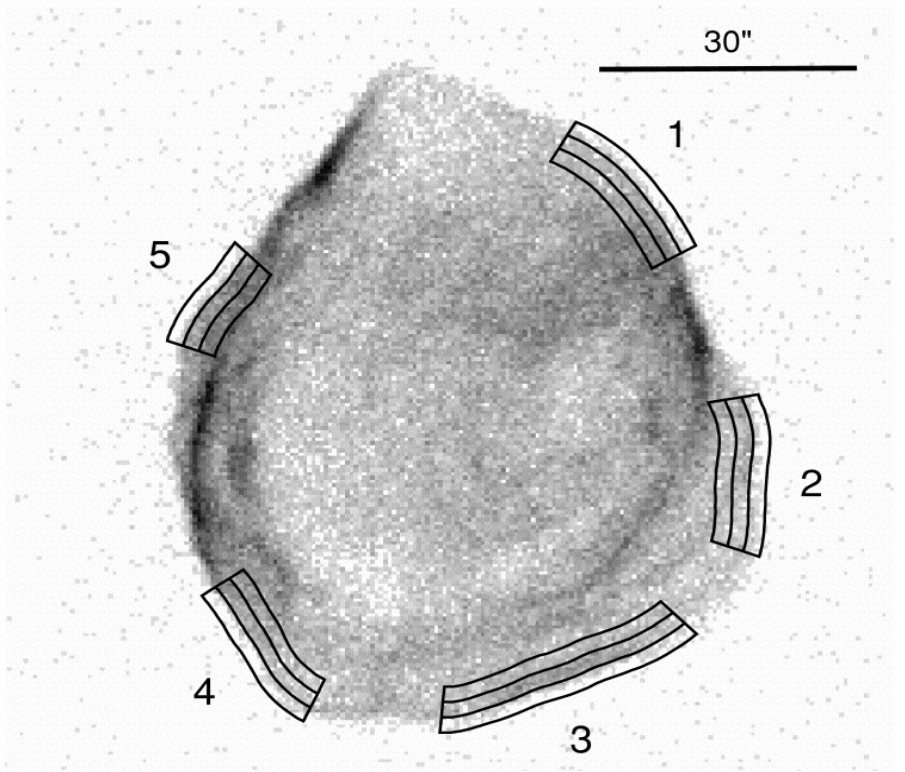

Fabry-Perot imaging spectr.

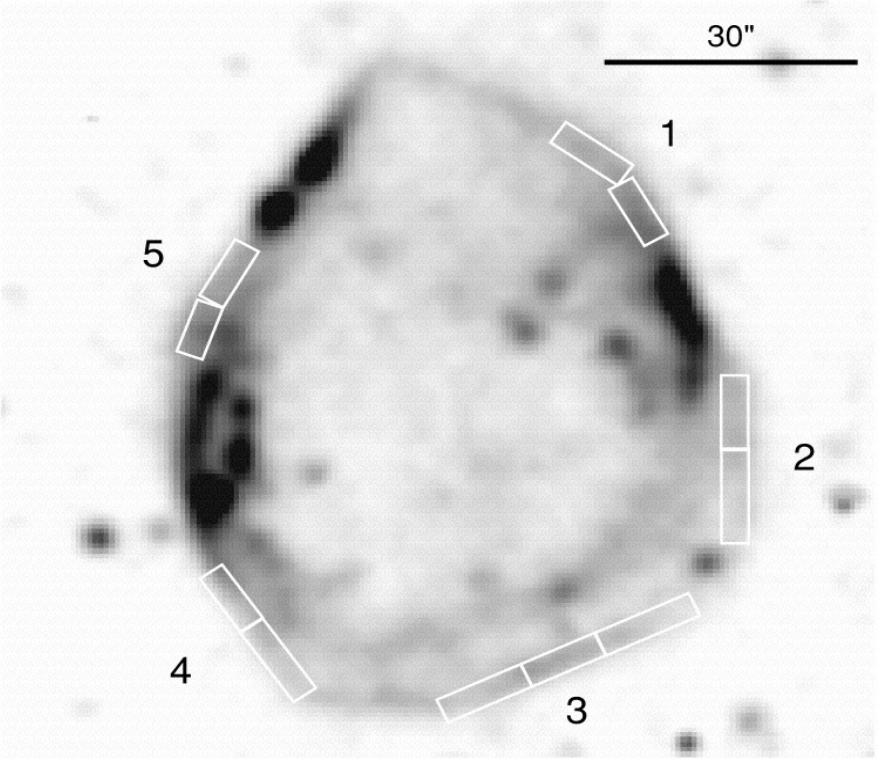

TABLE 2

RFP Hα Results for Selected Regions in the DEM L71 Blast Wave

	Hα Profile Fits		$(T_e/T_p)_0 = 1$		$(T_e/T_p)_0 = m_e/m_p$	
Aperture	$V_{\rm FWHM}$ (km s^{-1})	I_B/I_N	$V_{\rm shock}$ (km s^{-1})	kT_p (keV)	$V_{\rm shock}$ (km s^{-1})	kT_p (keV)
1	840^{+115}_{-100}	0.51 ± 0.06	1050^{+140}_{-130}	$1.29^{+0.38}_{-0.30}$	815^{+115}_{-100}	$1.29^{+0.38}_{-0.30}$
2	985^{+210}_{-165}	0.54 ± 0.09	1240^{+290}_{-210}	$1.81^{+0.95}_{-0.56}$	960^{+215}_{-165}	$1.81^{+0.90}_{-0.57}$
3	805^{+140}_{-115}	$0.49^{+0.07}_{-0.06}$	1005^{+170}_{-150}	$1.18^{+0.44}_{-0.32}$	775^{+140}_{-115}	$1.18^{+0.46}_{-0.32}$
4	735^{+100}_{-85}	0.66 ± 0.08	915^{+130}_{-105}	$0.99^{+0.29}_{-0.21}$	710^{+100}_{-80}	$0.98^{+0.29}_{-0.21}$
5	450 ± 60	$0.44^{+0.06}_{-0.05}$	555^{+75}_{-70}	$0.36^{+0.10}_{-0.09}$	430^{+60}_{-55}	$0.36^{+0.11}_{-0.09}$

SNRs: Coulomb interaction between electrons and ions

$$\Lambda_{ei} = \frac{3}{2}\frac{k_B(T_i - T_e)}{m_H}\left[1 + \left(\frac{4\,k_B T_e}{m_e c^2}\right)^{1/2}\right]\int_{z_0}^{\infty} \nu_{ei}\,\rho\,dz$$

$$\nu_{ei} \approx 2.44\times10^{21}\,\rho\,T_e^{-1.5}\times 20$$

$$g_0 = T_e/T_i \approx m_e/m_i$$

TABLE 3

AVERAGE N_H AND ABUNDANCES

Model	N_H ($\times10^{20}$ atoms cm^{-2})	O (dex)	Ne (dex)	Fe (dex)
$g_0 = 1$, planar.....	5.8 ± 1.8	$8.39^{+0.09}_{-0.12}$	$7.64^{+0.11}_{-0.15}$	$6.86^{+0.09}_{-0.11}$
$g_0 = m_e/m_p$, planar	6.0 ± 1.7	$8.40^{+0.10}_{-0.13}$	$7.66^{+0.11}_{-0.15}$	$6.86^{+0.11}_{-0.14}$
$g_0 = 1$, Sedov.....	7.1 ± 2.3	$8.41^{+0.10}_{-0.13}$	$7.78^{+0.07}_{-0.08}$	$6.83^{+0.09}_{-0.12}$
Combined	6.3 ± 1.9	$8.40^{+0.09}_{-0.12}$	$7.70^{+0.10}_{-0.14}$	$6.86^{+0.09}_{-0.11}$

SNRs and their X-ray spectra:

Time dependent ionization: $g_0 = T_e / T_i \approx m_e / m_i$

Bremsstrahlung continuum provides direct measure of the electron temperature.

Electrons interact with ions by Coulomb collisions, equilibrium when: $T_e = T_i$

Rakowski + 2005

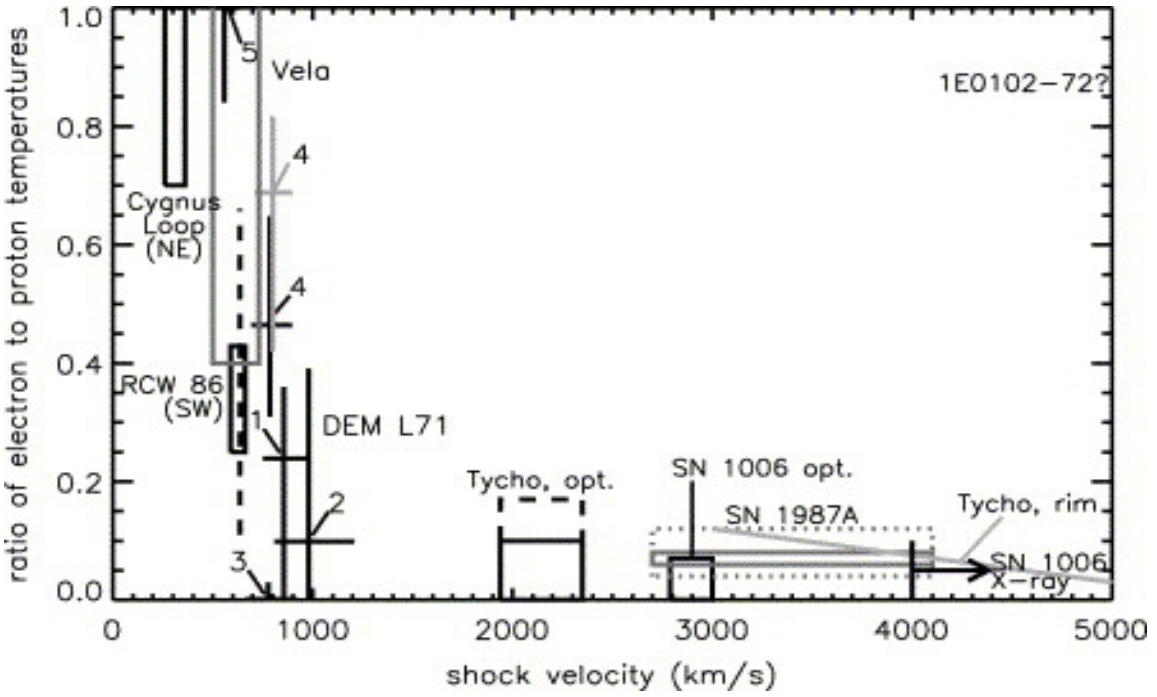

SNRs and their hard X-ray spectra:

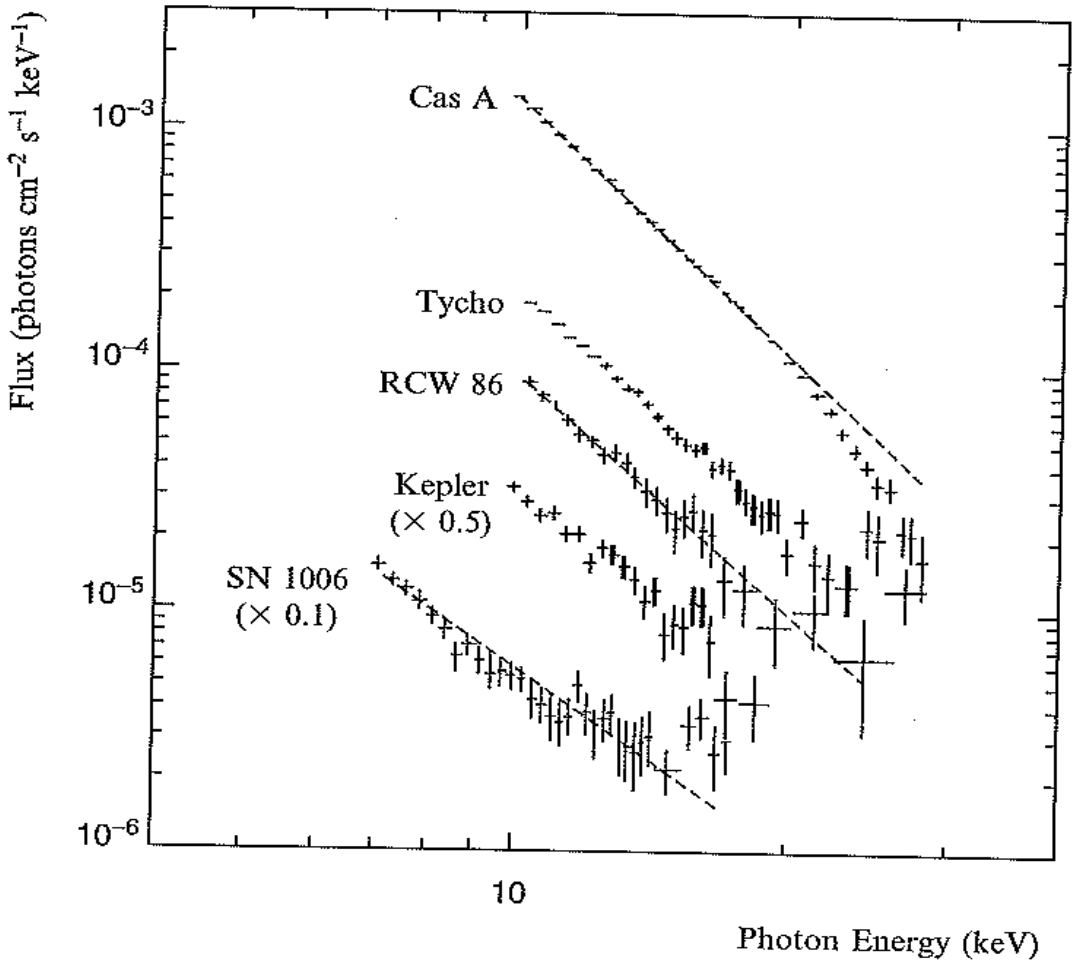

Fig. 17.11 RXTE PCA spectra of five historical SNRs with hard nonthermal tails probably produced by synchrotron emission from TeV electrons. Each spectrum is characterized by a power law with spectral index of approximately 2 [114]

Kinematics SNRs:

Average shock velocity 5000 km/s at a distance 3 kpc.
Average angular expansion rate is 0.35 per year.

The X-ray ejecta are moving twice as fast as the cospatial radio knots.

Doppler mapping of Cas A;
Willingale + 2002.

Si and S emission from narrow shell with radius 100-150 arcsec, Fe-K emission is confined in two large clumps, expanding faster with radius up to 170 arcsec.

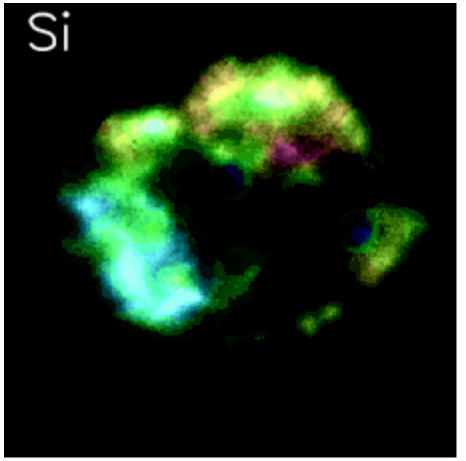

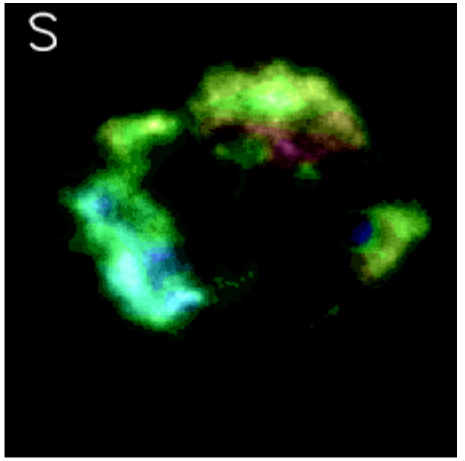

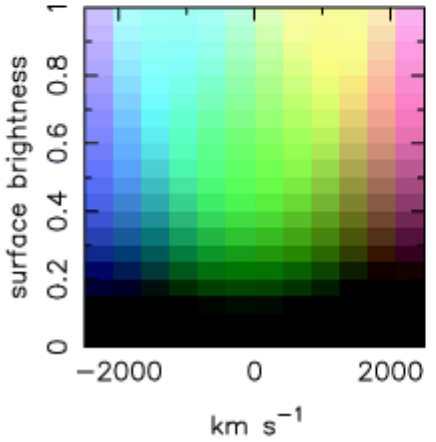

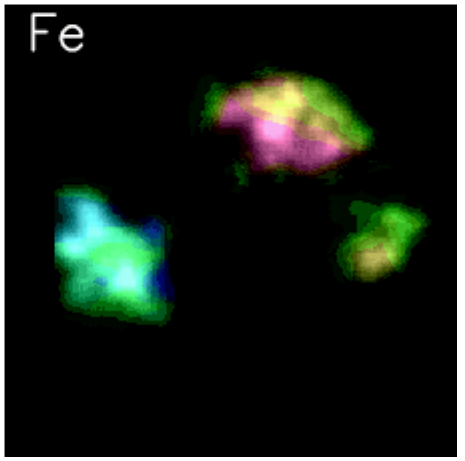

X-ray emission from SNe is a rarity:

Only most luminous such objects are detectable: $L_x > 10^{39}\, erg/s$
Compared with hundreds of SNe detected in optic, only 30-40 have been detected in X-rays.

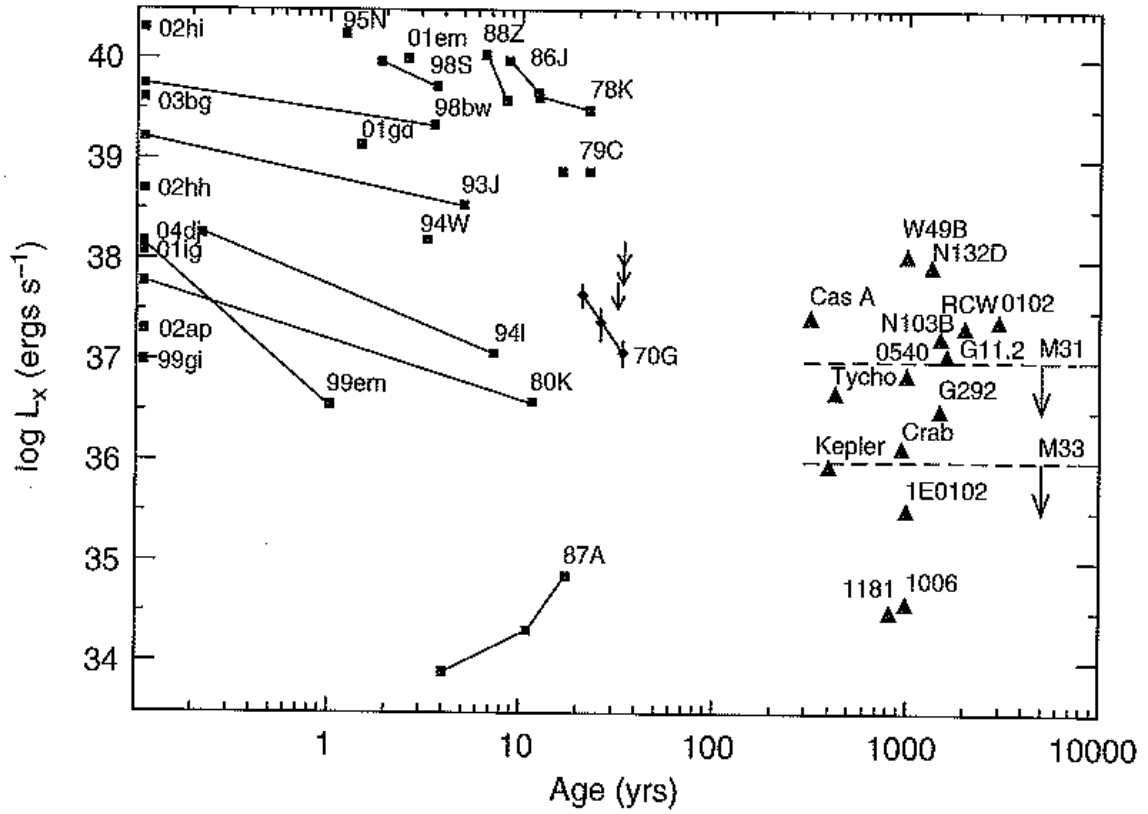

Fig. 17.14 X-ray light curves (0.32 keV) band of all SNe detected to date (*filled squares*). A range of behaviors is observed, from flat to dropping steeply. Only SN 1987A shows increasing luminosity [73]. The figure suggests that the luminosities of historical SNRs (*filled triangles* on the right) can be extrapolated from the SN luminosities

SN 1987 A: the lowest X-ray luminosity supernova.

50 kps in the LMC. January 27, 1987 – at that time only X-ray instruments were HEXE and Ginga.
5 months after explosion – no signal....
6 months after explosion – hard X-rays detected independently.

In 1990 – ROSAT observed:

$$L_x \sim 10^{34}\, erg/s$$

at 0.2-2.4 keV.

Chandra saturated on:

$$L_x \sim 3.6 \times 10^{36}\, erg/s$$

at 0.5-2.0 keV.

Forward shock is now propagating beyond a density peak of the interior ring.

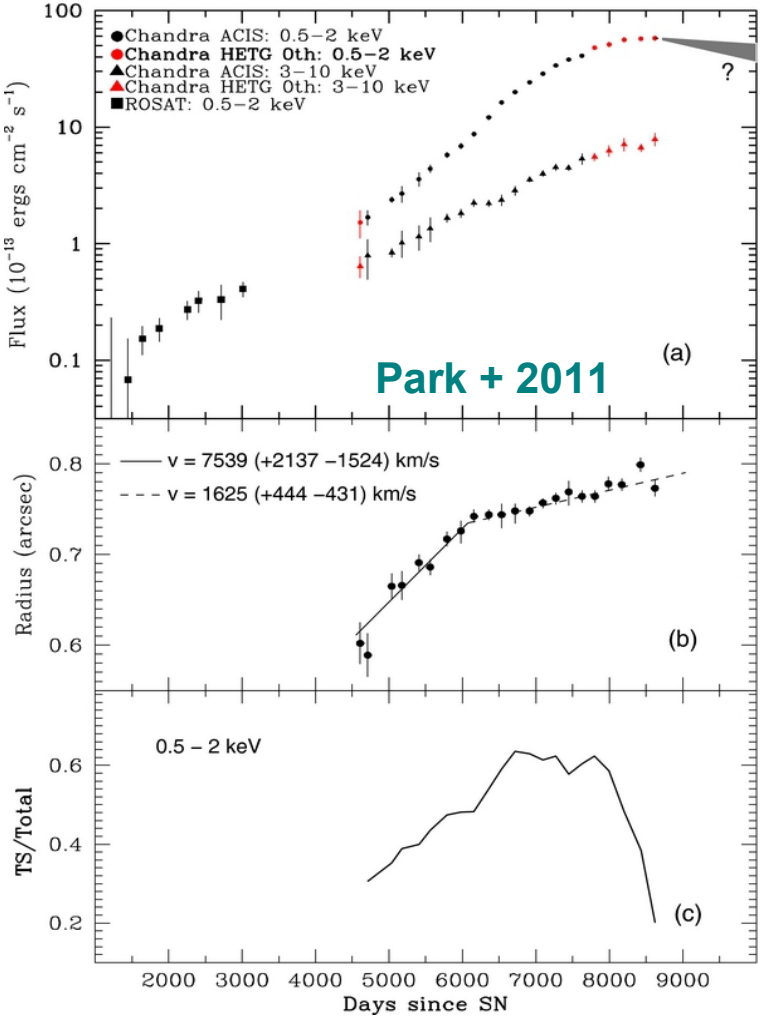

ISM found by Trumpler in 1930:

The transmitted fraction of an X-ray beam with intensity I_0:

$$I = I_o \exp[-\sigma(E) N_H]$$

$$\sigma_K = 4\sqrt{2}\,\alpha^4 Z^5 \sigma_T \left(\frac{m_e c^2}{E}\right)^{7/2}$$

$$\sigma(E) = \sum_i \frac{n_i}{n_H} \sigma_i(E)$$

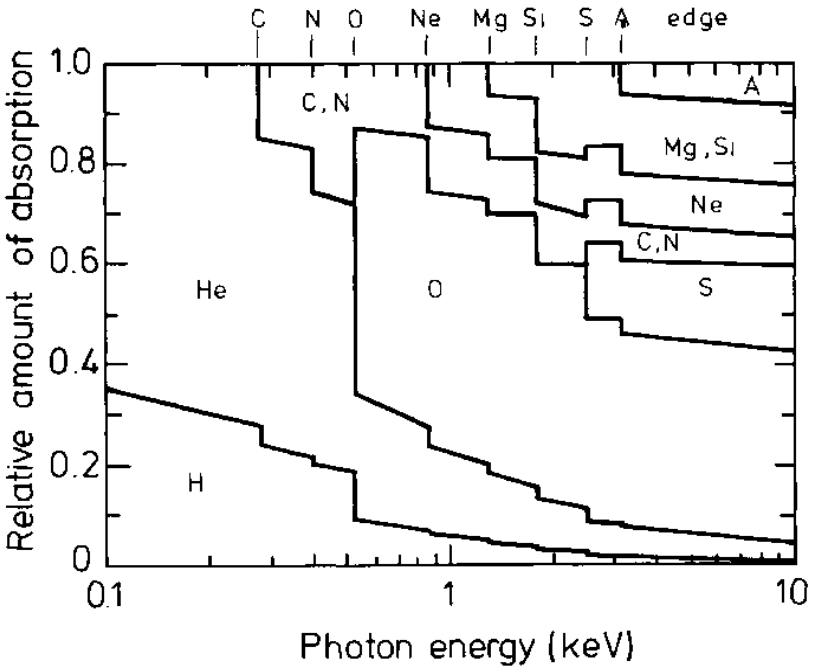

Fig. 2. Relative importance of different elements in the interstellar medium for the absorption of soft X-rays (Seward, 1975)

ISM in X-rays:

Tanaka + 1977

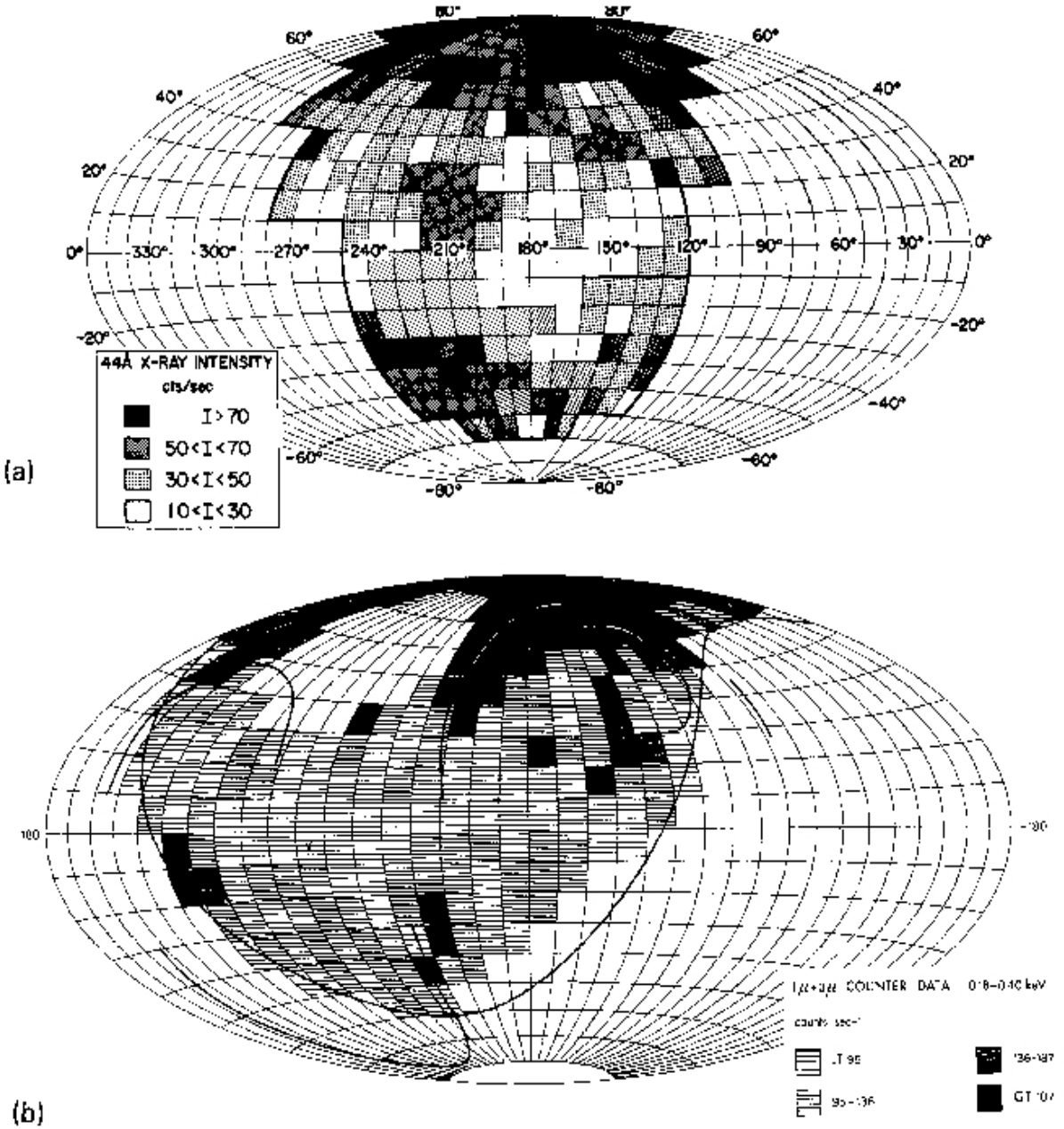

ISM in X-rays:

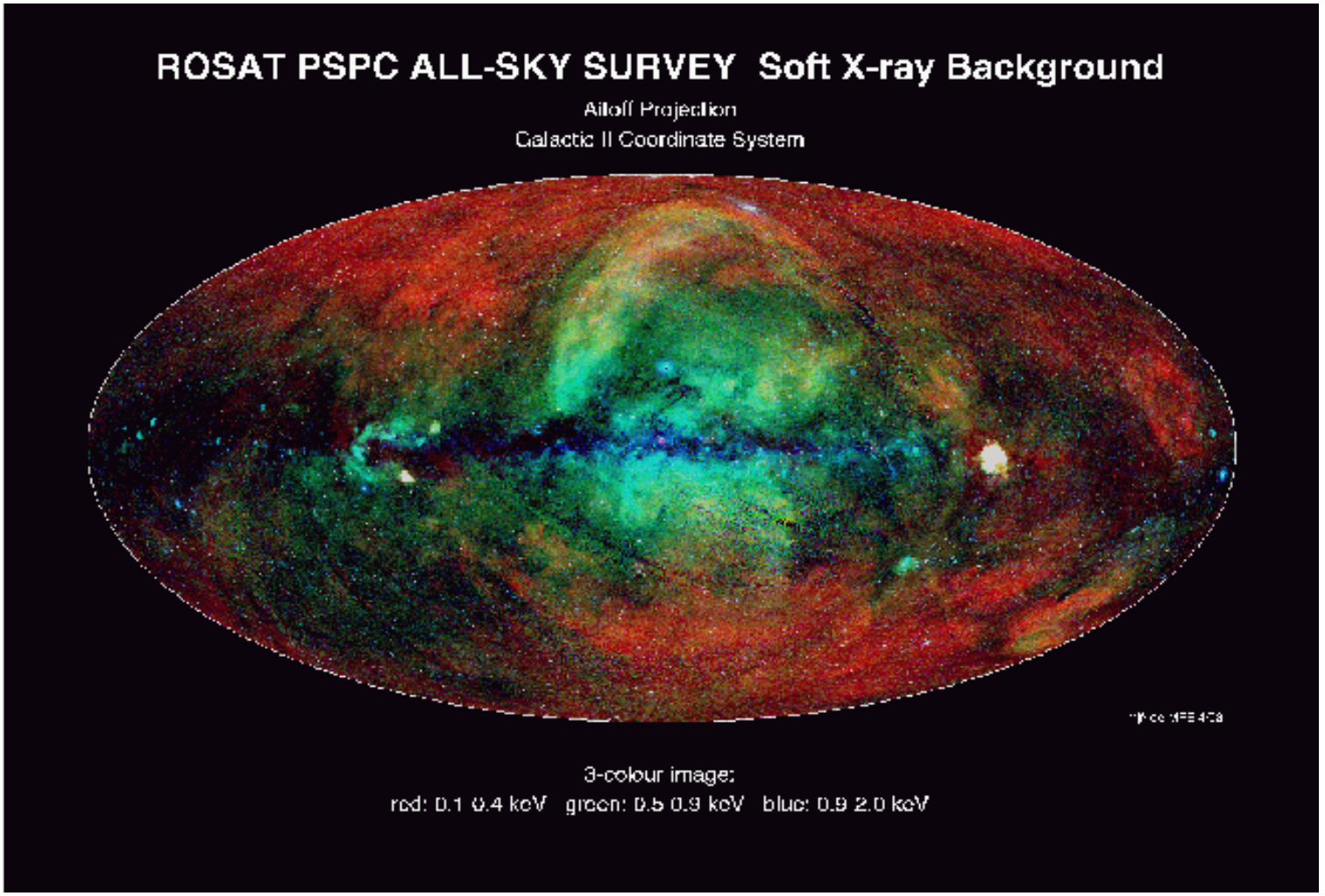

Multispectral X-ray view of the soft X-ray background as seen in the ROSAT PSPC. Galactic center is at l=0°.

The Galactic Center:

The center of our Galaxy lies within the Sagittarius at a distance of ~ 8 kpc, behind a large column density of gas and dust. Galactic nucleus a factor of 100 closer than next in M31.

First, nonthermal compact radio source Sgr A* was detected.

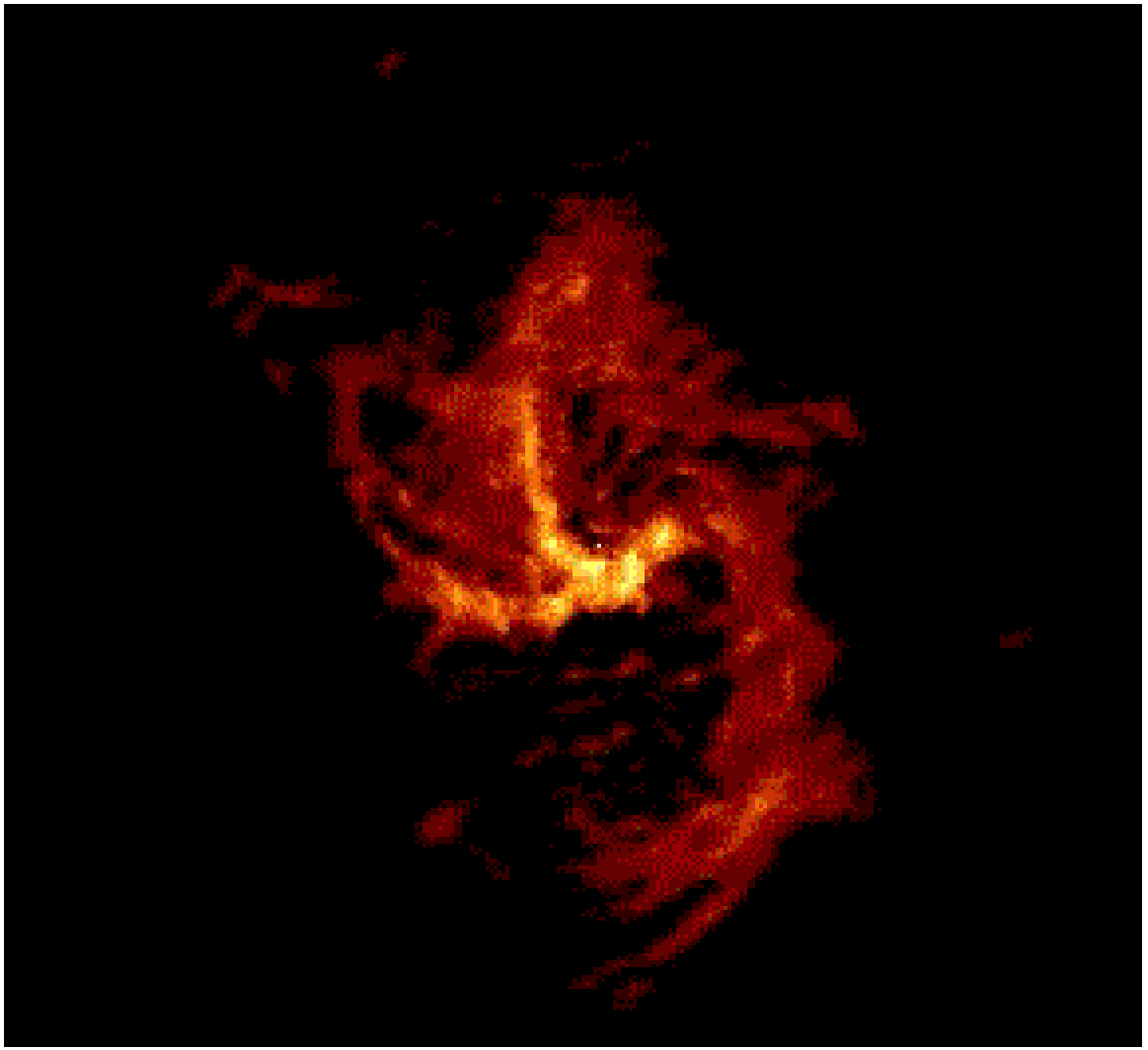

The Galactic Center:

Near-infrared observations revealed orbital motions of stars in the vicinity of Sgr A* allowing to determine:

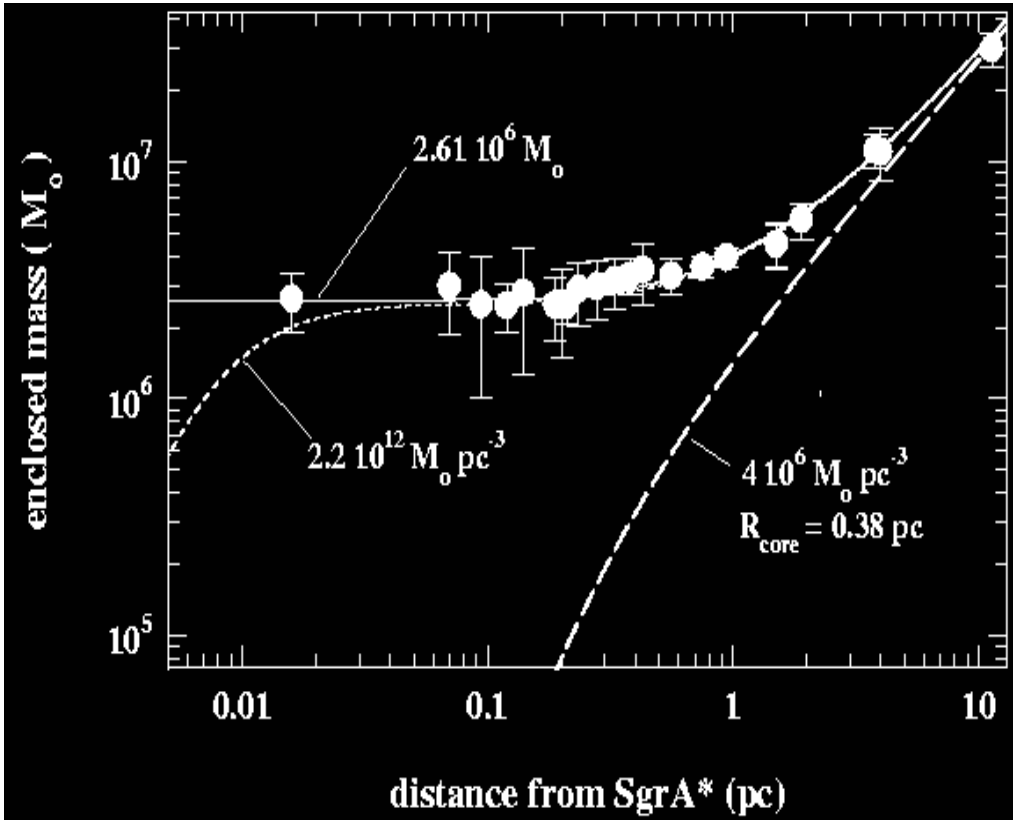

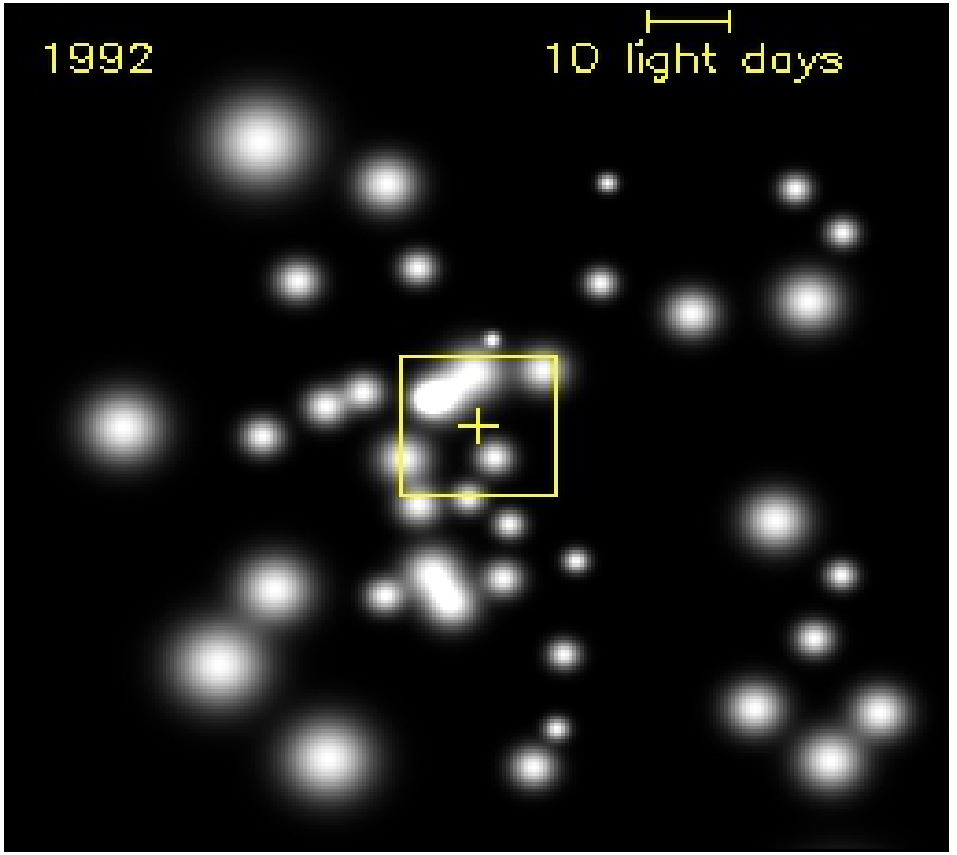

$$M_{BH} \sim 4 \times 10^6 M_{Sun}$$

The Galactic Center:

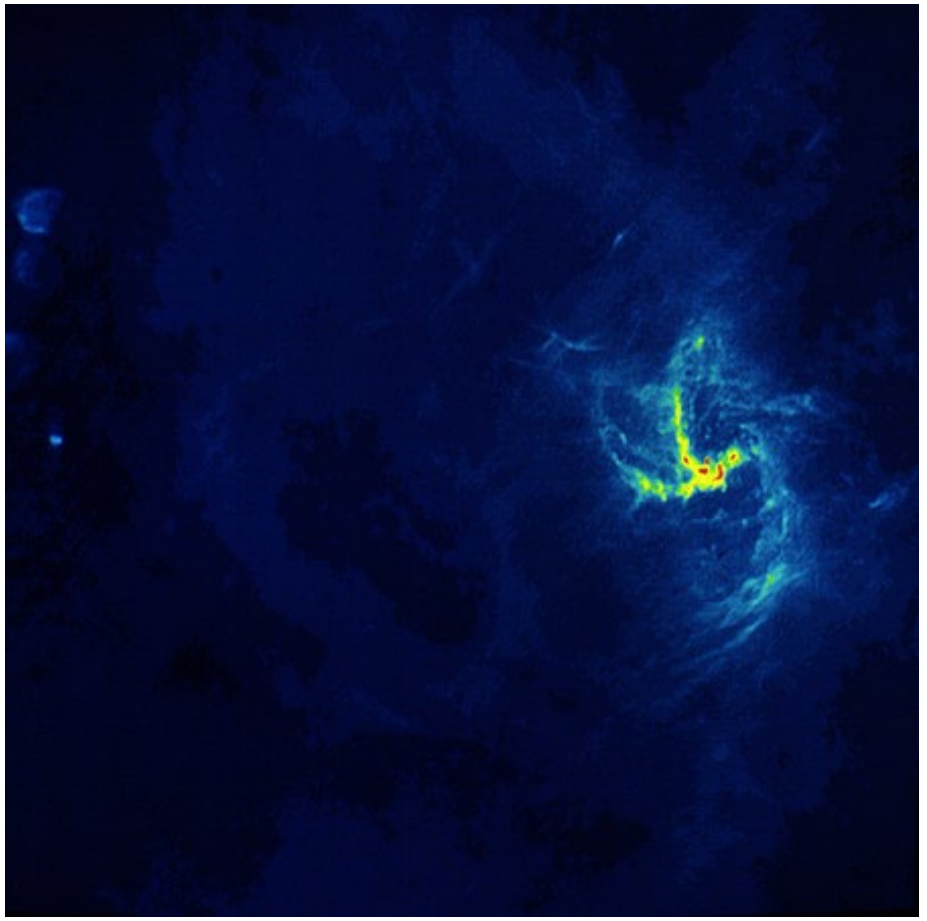

Radio image of Sgr A*

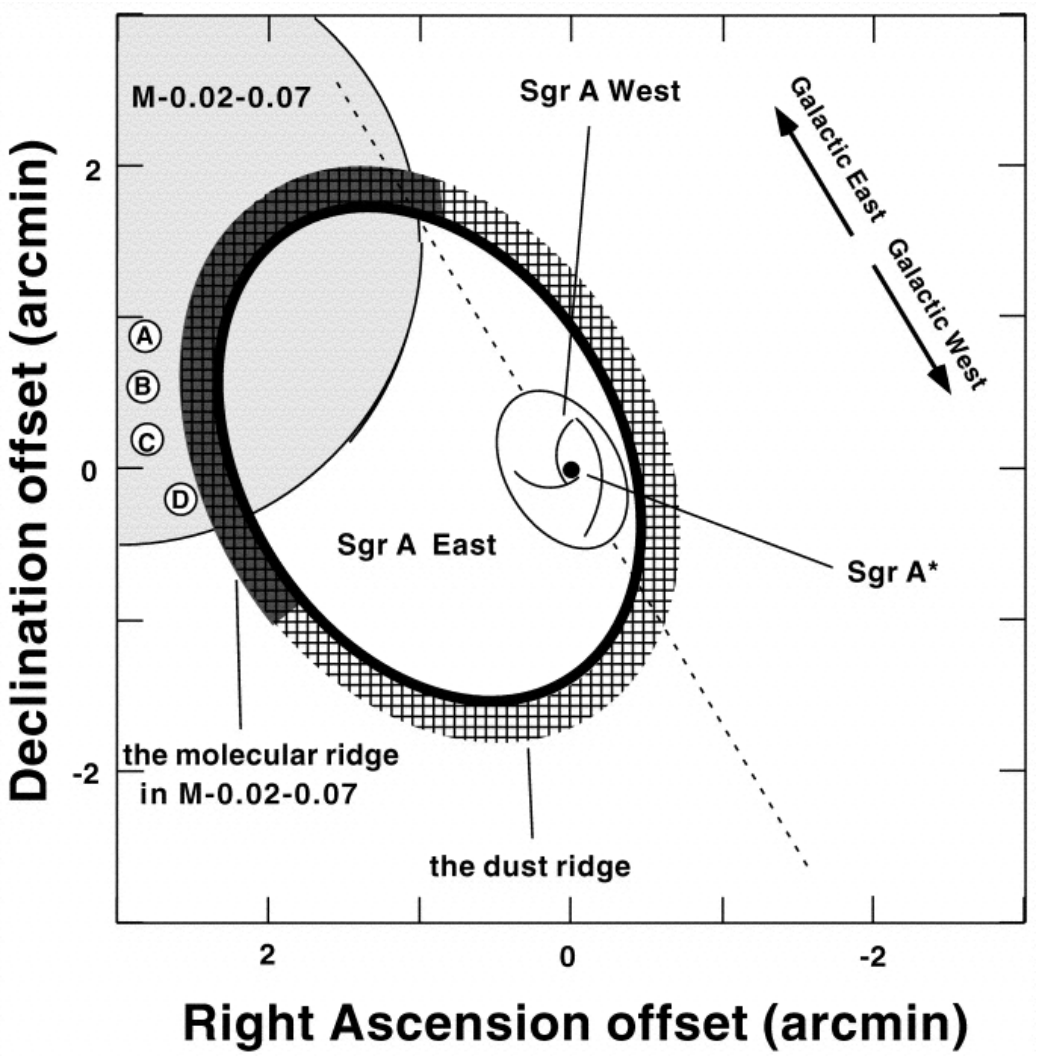

The Galactic Center:

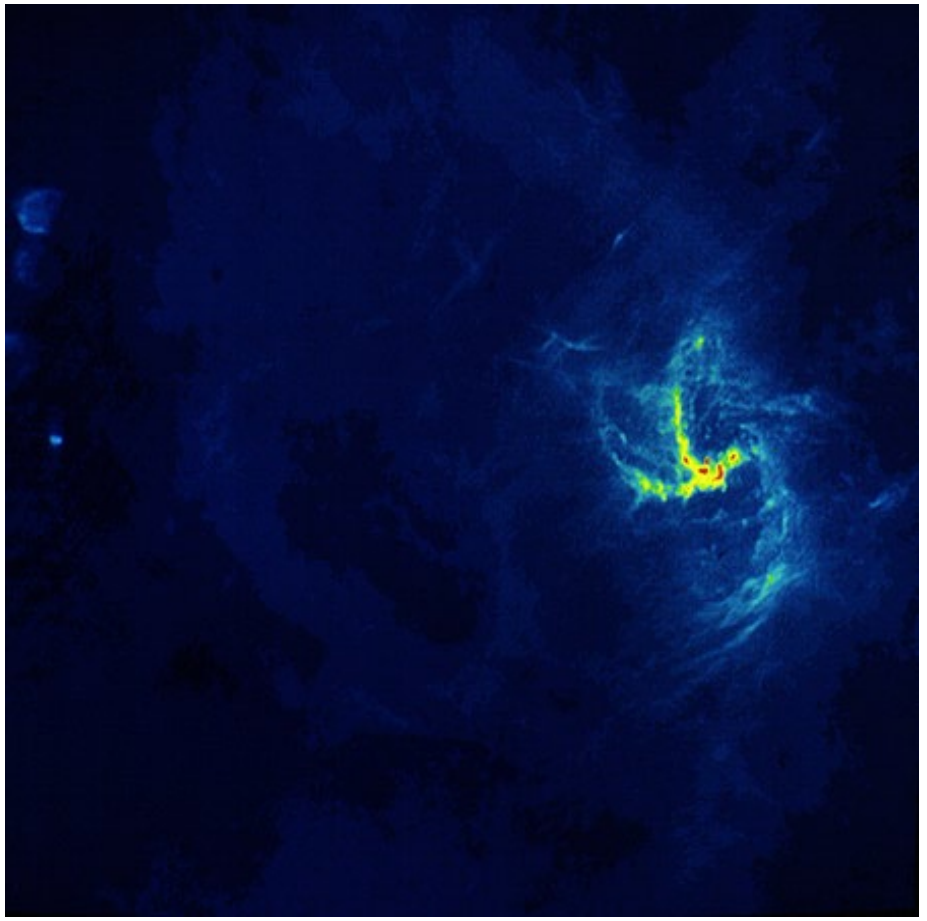

Radio image

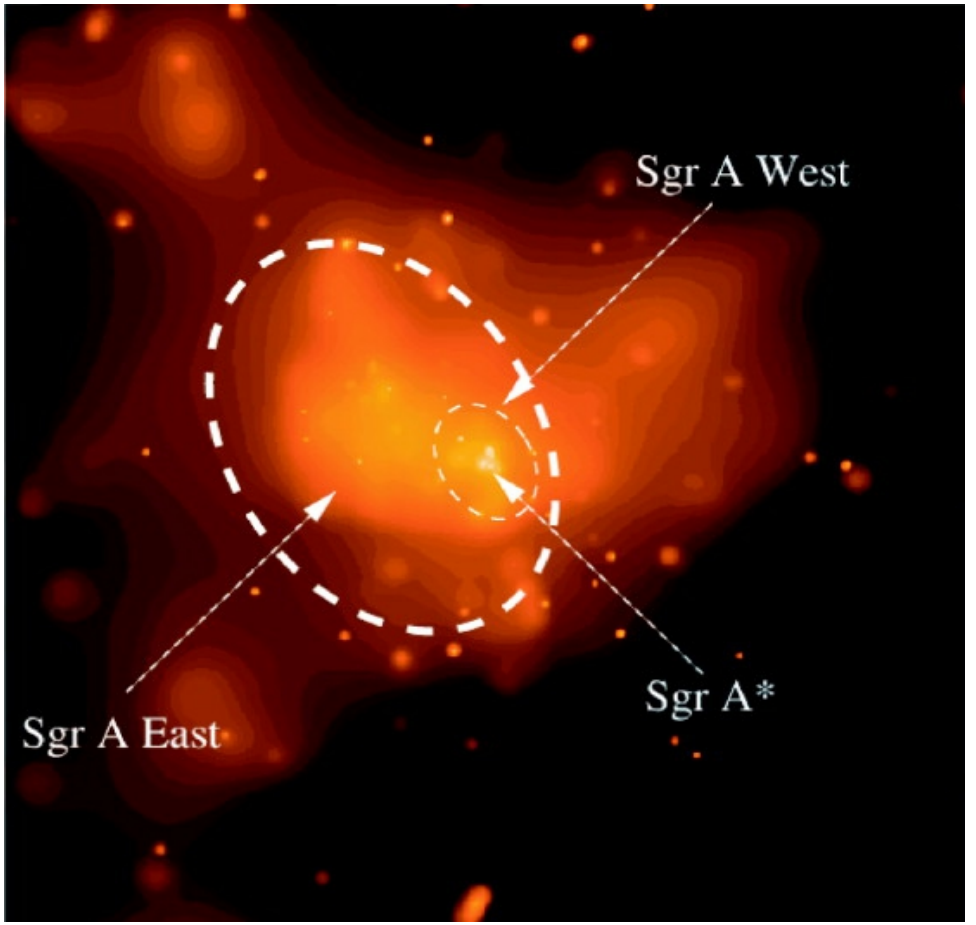

Chandra 1.5-7 keV
Maeda + 2002

The Galactic Center:

Sgr A East – multiple supernova eruption,
Chandra and XMM-Newton indicate that total energy of the hot plasma is smaller than one SN:

$$E \approx 1.5 \times 10^{46} erg$$

The Galactic Center:

Sgr A East – multiple supernova eruption,
Chandra and XMM-Newton indicate that total energy of the hot plasma is smaller than one SN:

$$E \approx 1.5 \times 10^{46} erg$$

Chandra Maeda + 2002

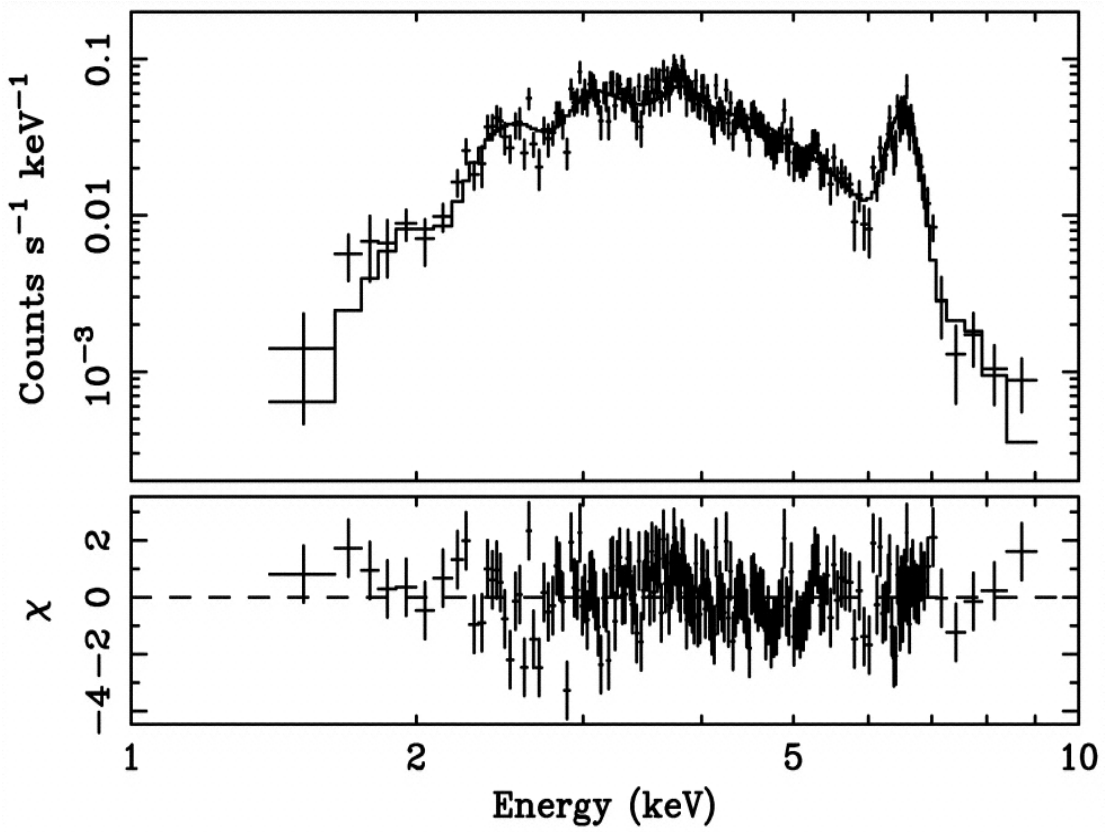

TABLE 1

BEST-FIT PARAMETERS TO THE SGR A EAST SPECTRUM FITTED WITH A THERMAL BREMSSTRAHLUNG WITH FOUR GAUSSIANS

Continuum	
Parameter	Value
N_H ($\times 10^{22}$ cm^{-2})	9.4 (8.7–10.2)
kT_e (keV)	3.0 (2.6–3.5)

Emission Lines			
Line Energy (keV)	Line ID (keV)[a]	I [10^{-5} photons cm^{-2} s^{-1}][b]	EW (eV)[c]
2.49 (2.45–2.53)	S XV (2.45)	0.9 (0.5–1.4)	140
3.16 (3.10–3.23)	Ar XVII (3.14)	1.1 (0.7–1.6)	92
3.85 (3.81–3.88)	Ca XIX (3.90)	2.2 (1.7–2.6)	173
6.69 (6.67–6.71)	Fe XXV (6.67)	12.2 (11.2–13.2)	3100

$$EW\left(Fe\,XXV\right) = 3.1\,keV$$

The Galactic Center:

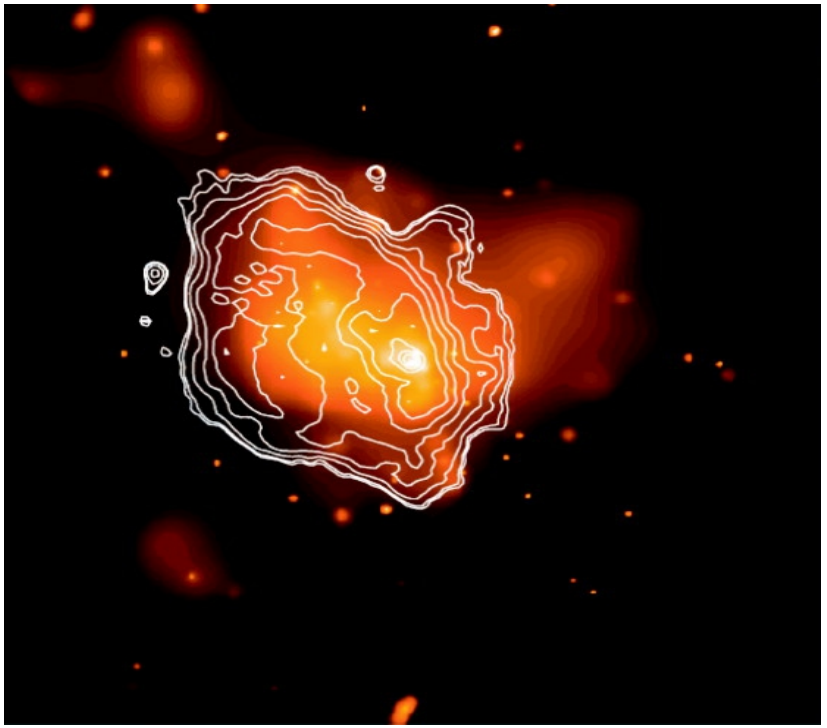

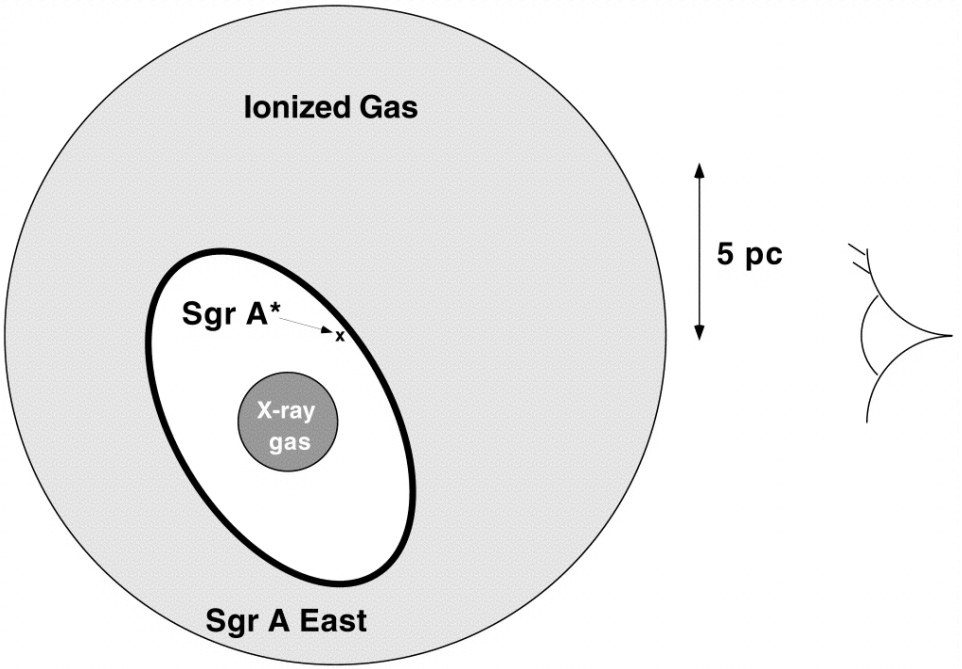

Iron is overabundant Z~ 3.5.
The existence of ionized halo surrounding Sgr A* supports the scenario that Sgr A* experienced active galactic nucleus (AGN) activity in the recent past.
X-ray luminosity is only about 2.2 x 10^{33} erg/s within the radius of 1.5" – if active 11 orders of magnitude less than L_{Edd}.

The Galactic Center:

Chandra exposure of the ~ 1.4" region consistent with Bondi accretion radius of 2.6×10^6 Solar masses BH.

Spectral fitting: power law with photon index:

$$\Gamma \approx 2.7$$
$$kT \approx 1.9\, keV$$
$$N_H \approx 10^{23}\, cm^{-2}$$

0.5 Msec Chandra, Baganoff + 2001

The Galactic Center:

Flares with duration about 10 ks.
Flux rise by a factor of about 6~30.

Spectra of non-flaring region: Porquet + 2008

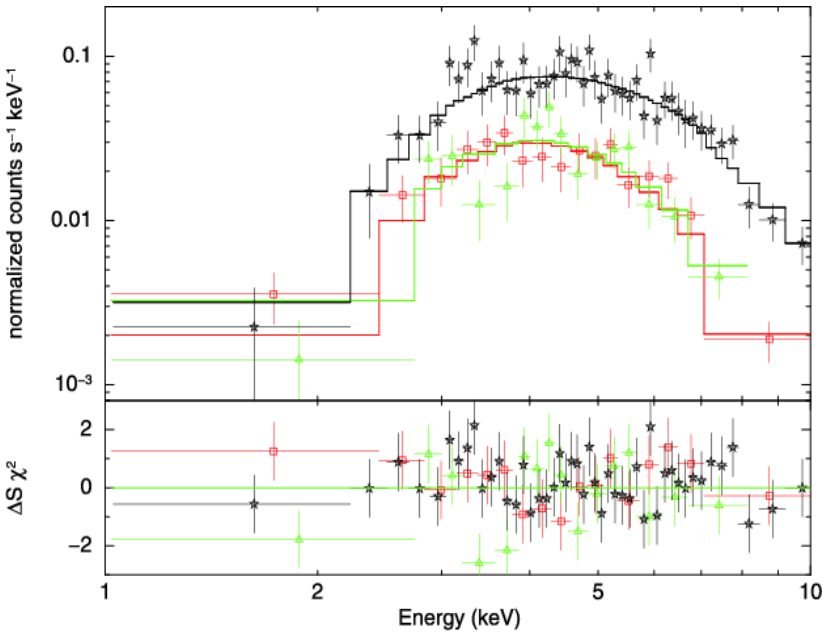

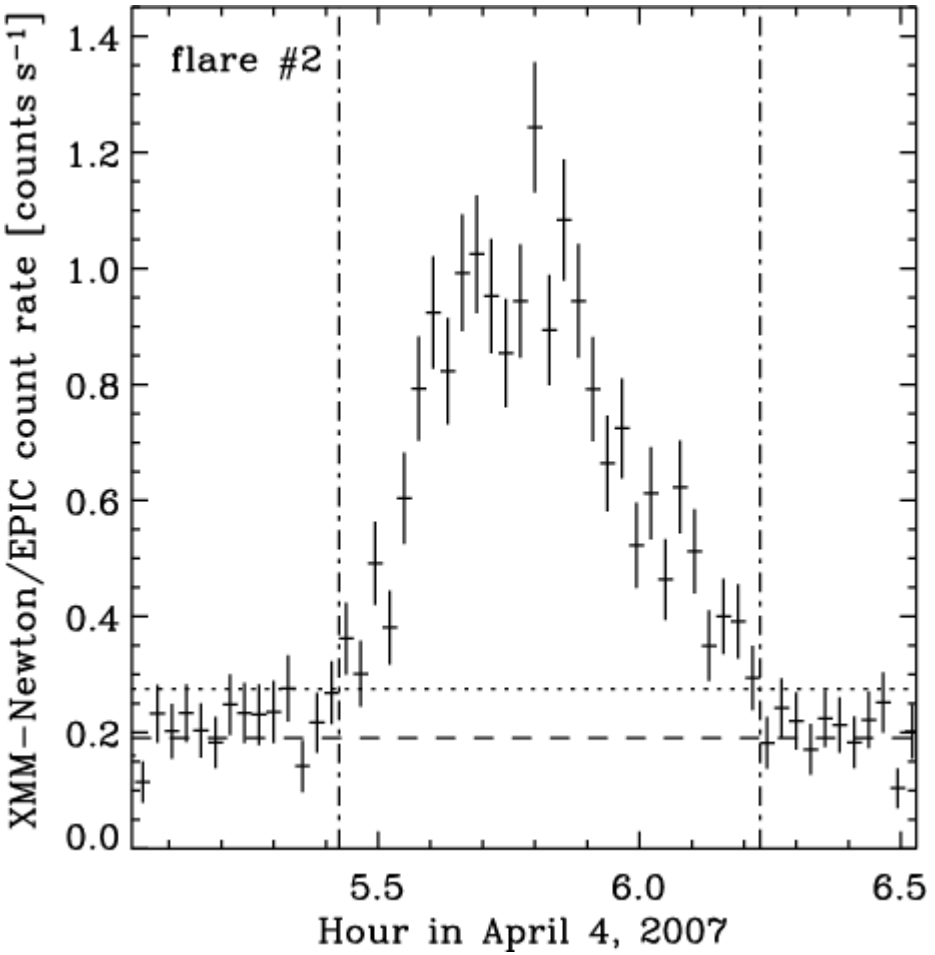

The Galactic Center:

Ponti + 2010, XMM- Newton observations 2000-2009 (1.2 Ms) of the region within 15 arcmin from Sgr A*.

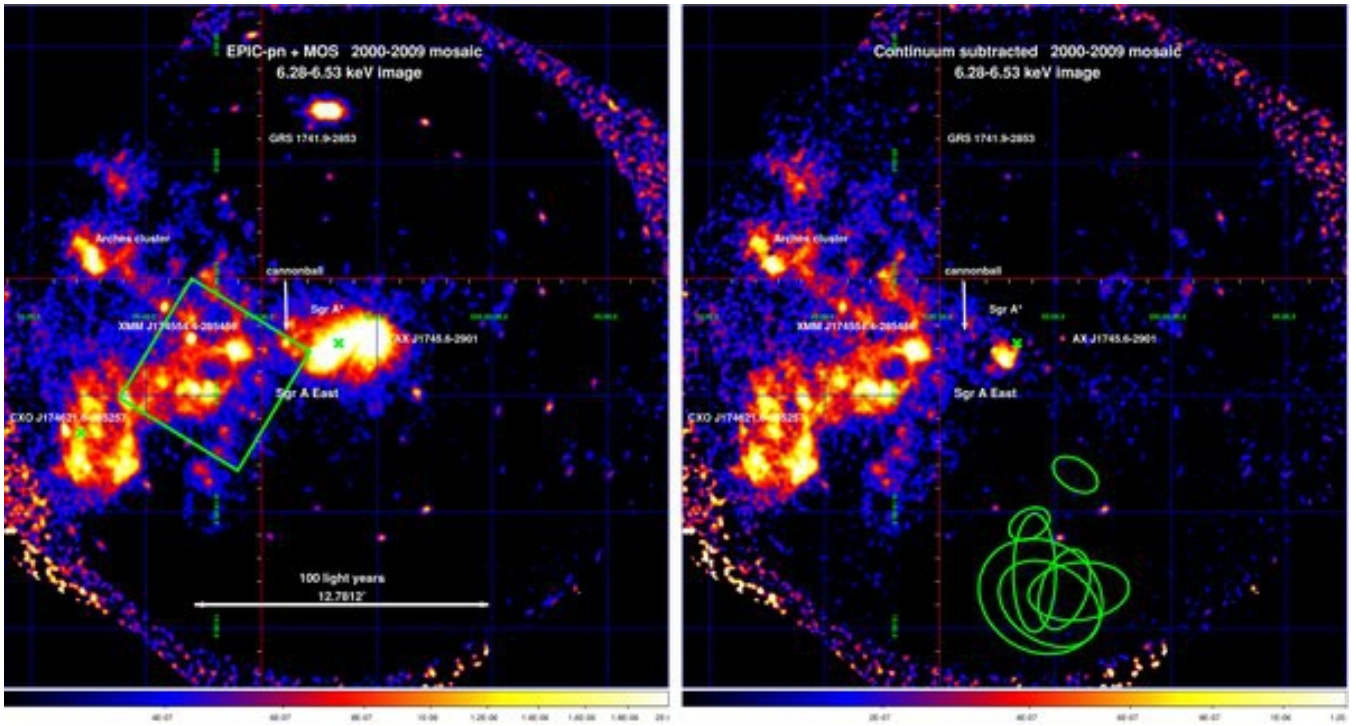

Continuum – power law fitting with photon index = 2.
Most of the contribution due to point sources is removed.

The Galactic Center:

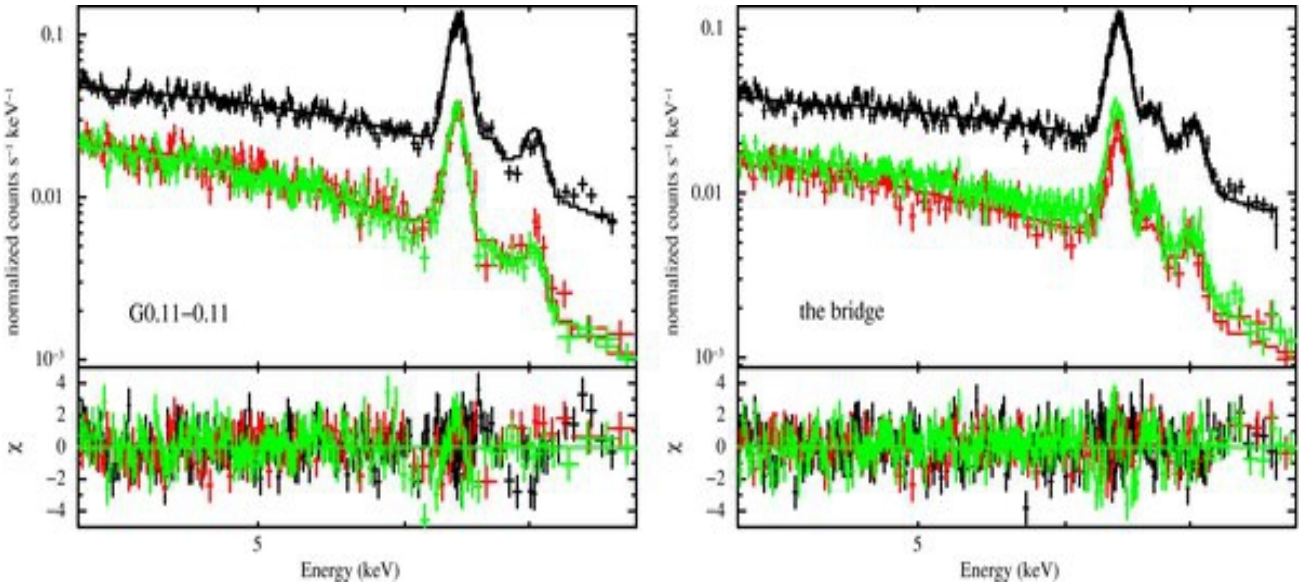

Continuum subtracted map (CS)

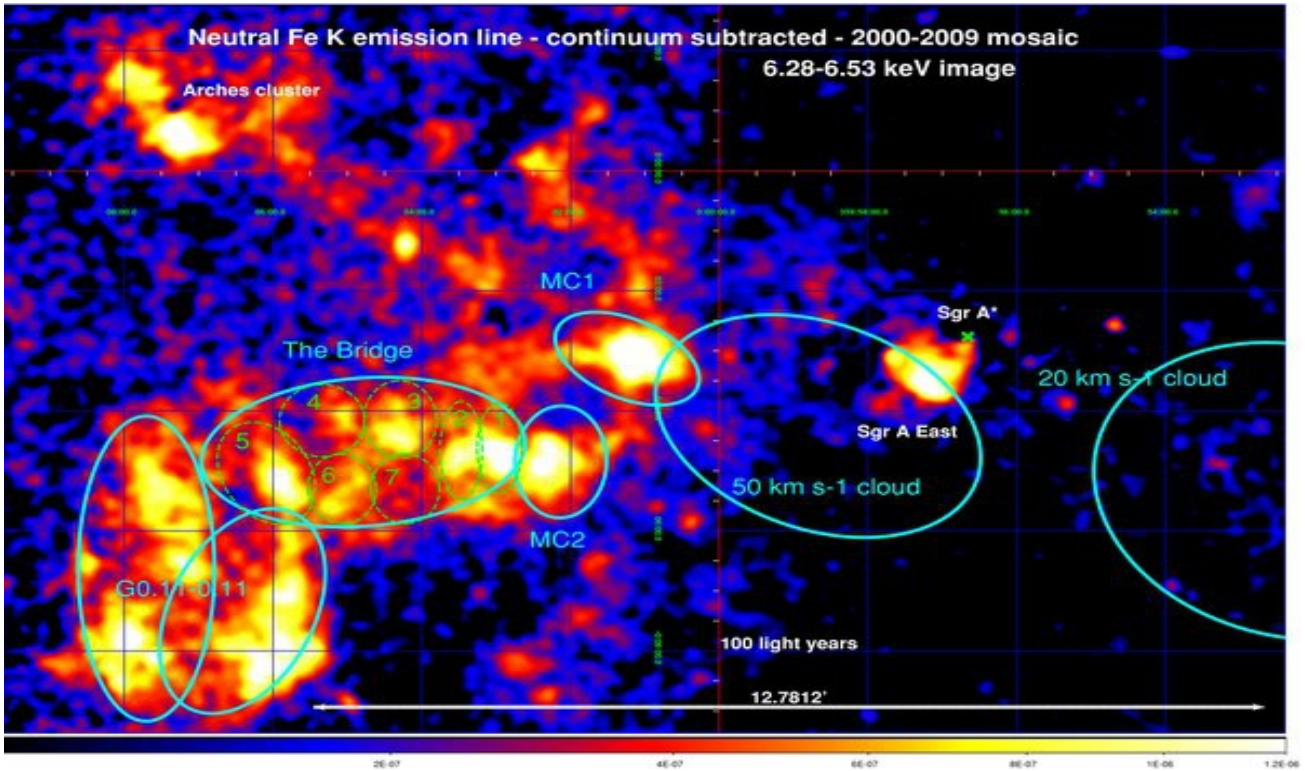

The Galactic Center:

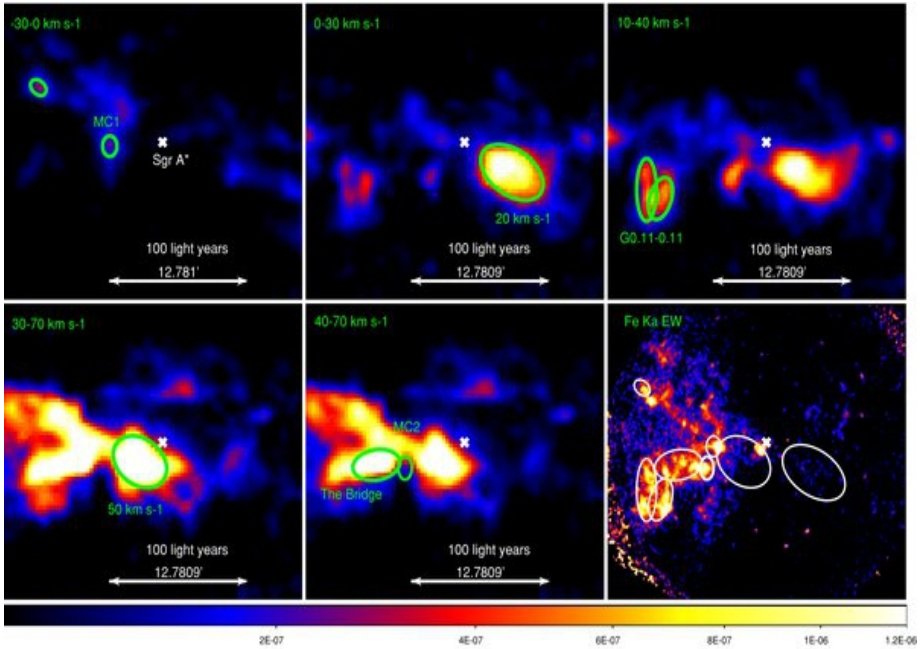

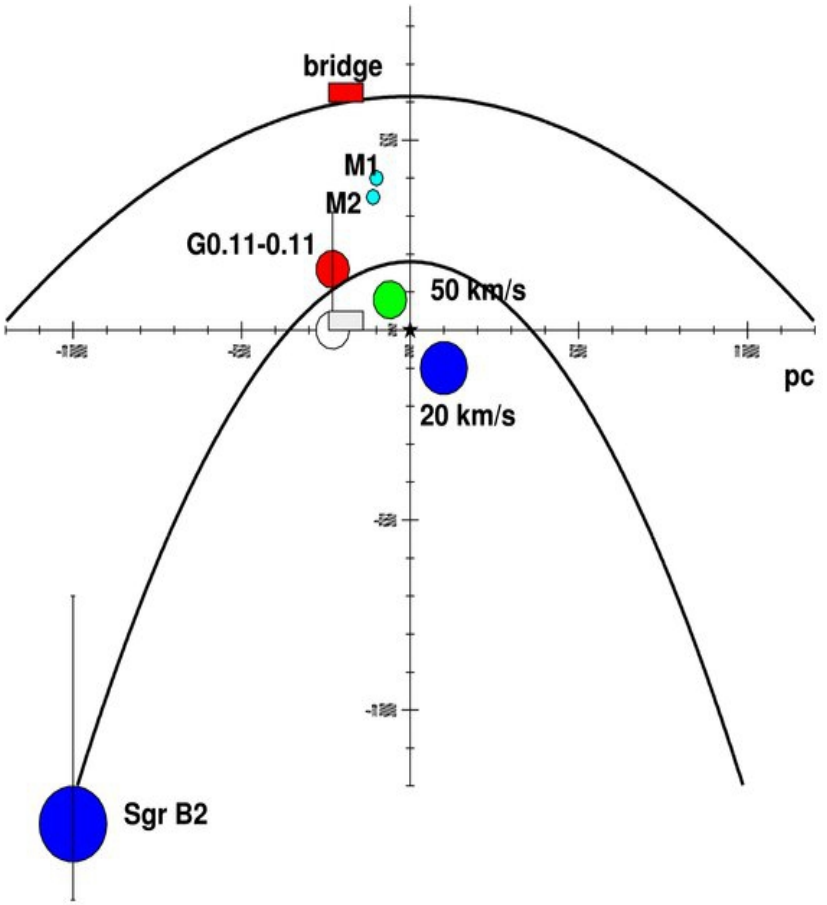

Ponti + 2010
Line emission as an echo
from past activity of X-ray source

Face – on view of Galactic Center

The Galactic Center:

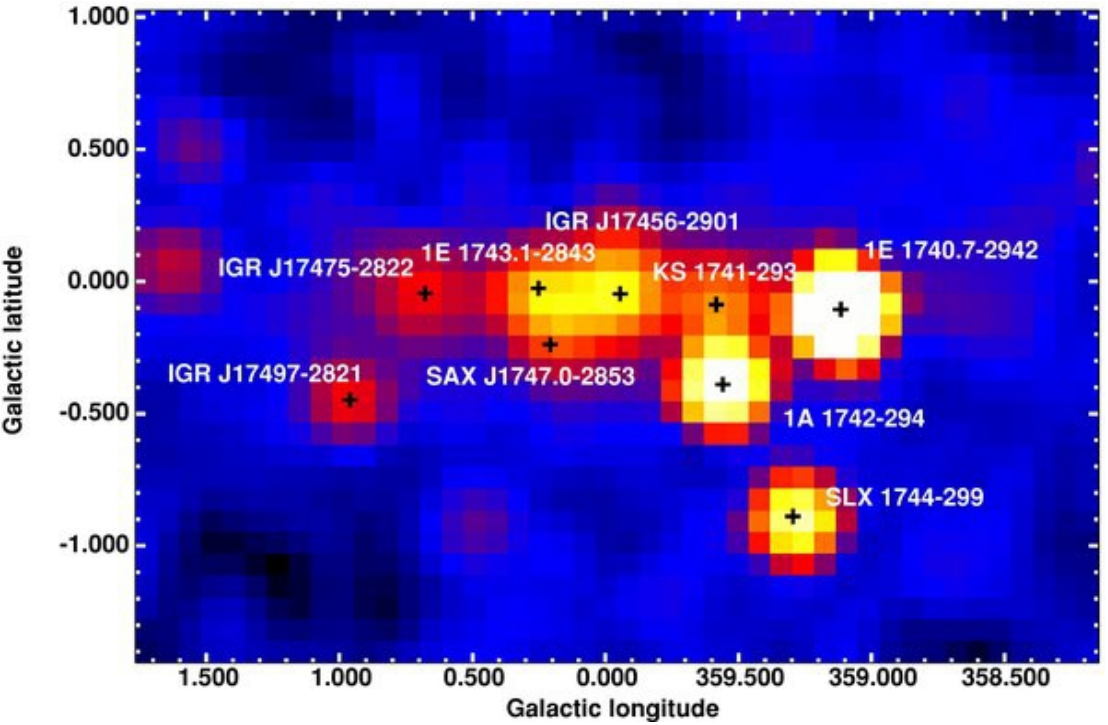

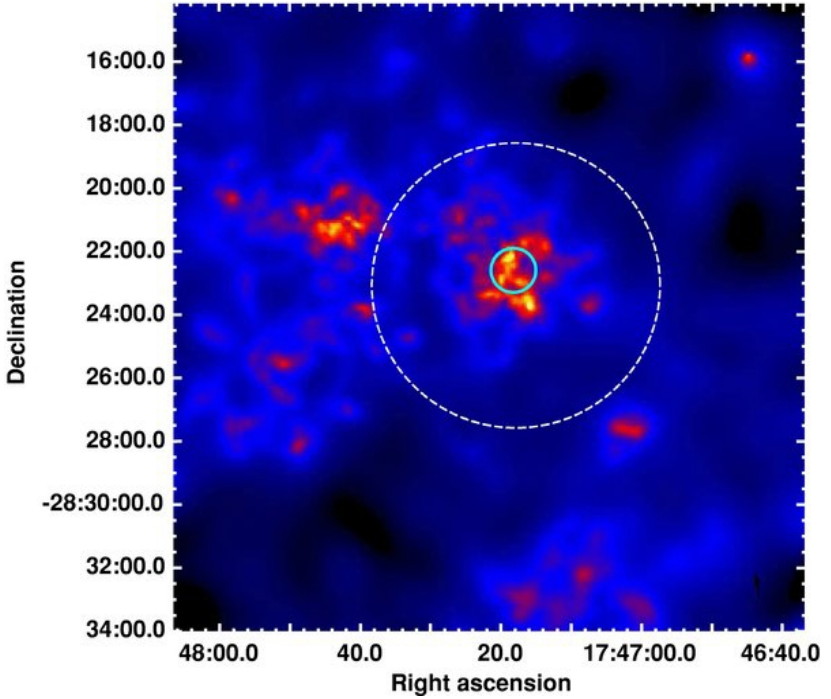

Integral 20-40 keV
Sgr B2 – IGR J17475

XMM/MOS in Fe line image. Blue circle best fit position with 90 %.

Terrier + 2011

The Galactic Center:

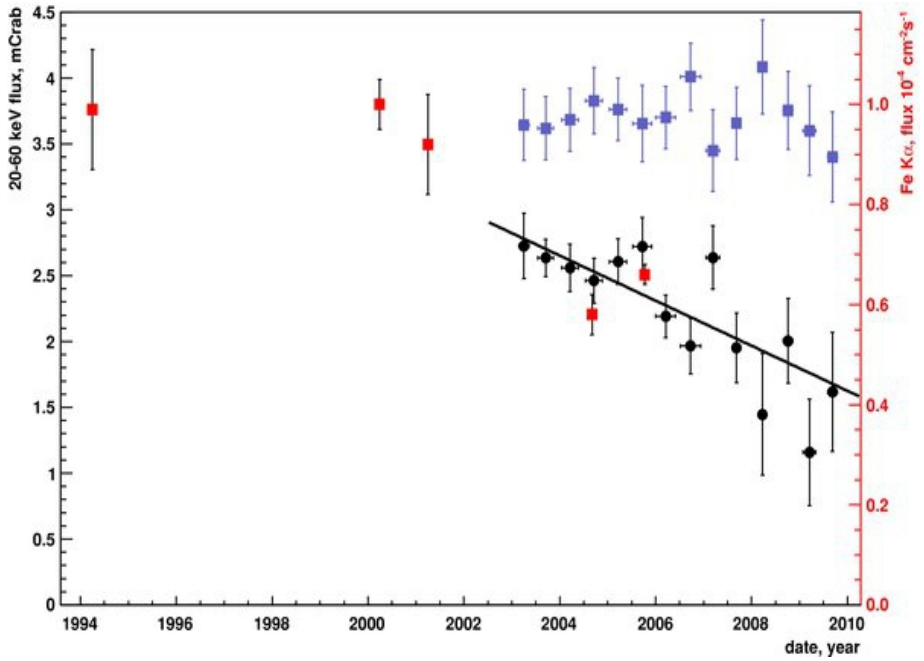

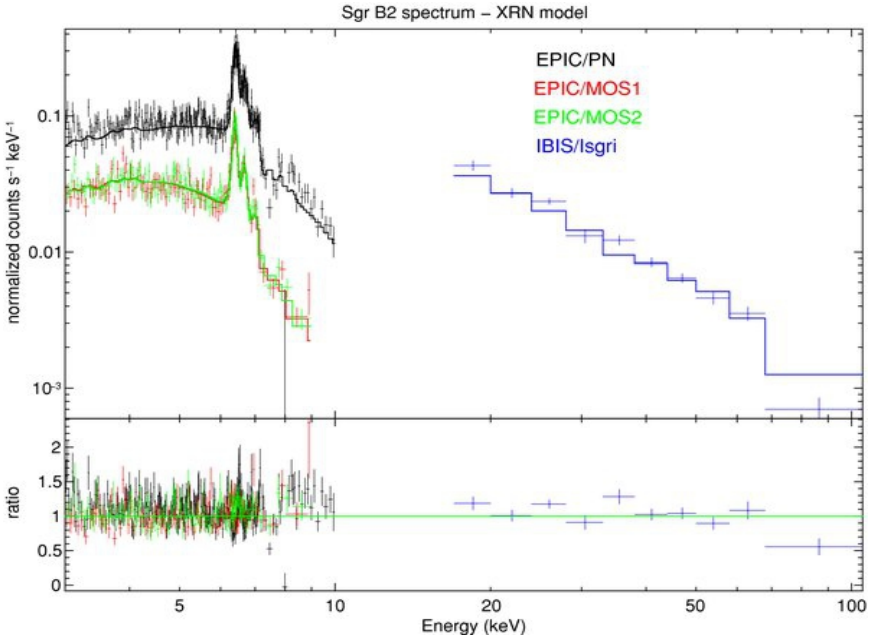

Integral – black ,
Chandra, XMM – red ,
Calibration object – blue.

The Galactic Center:

Yun-Wei Yu + 2011

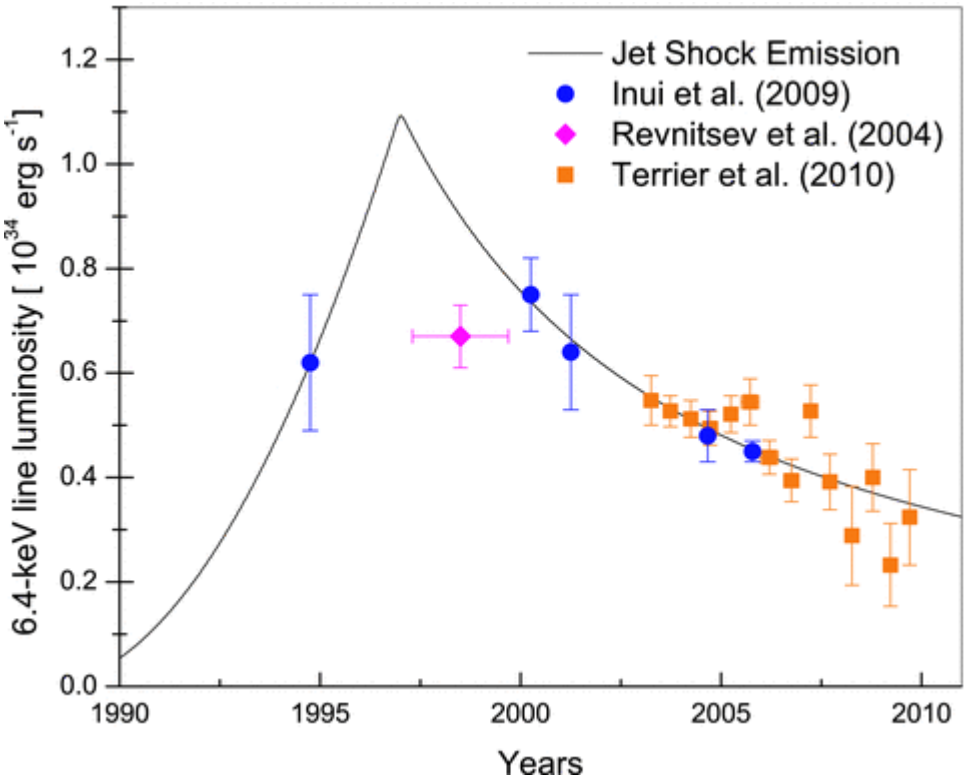

The observational luminosity data of the 6.4 keV line emission from the Sgr B2 cloud and an illustrative fitting (solid line).

The Galactic Center:

Różańska + 2015
Shcherbakov + 2010

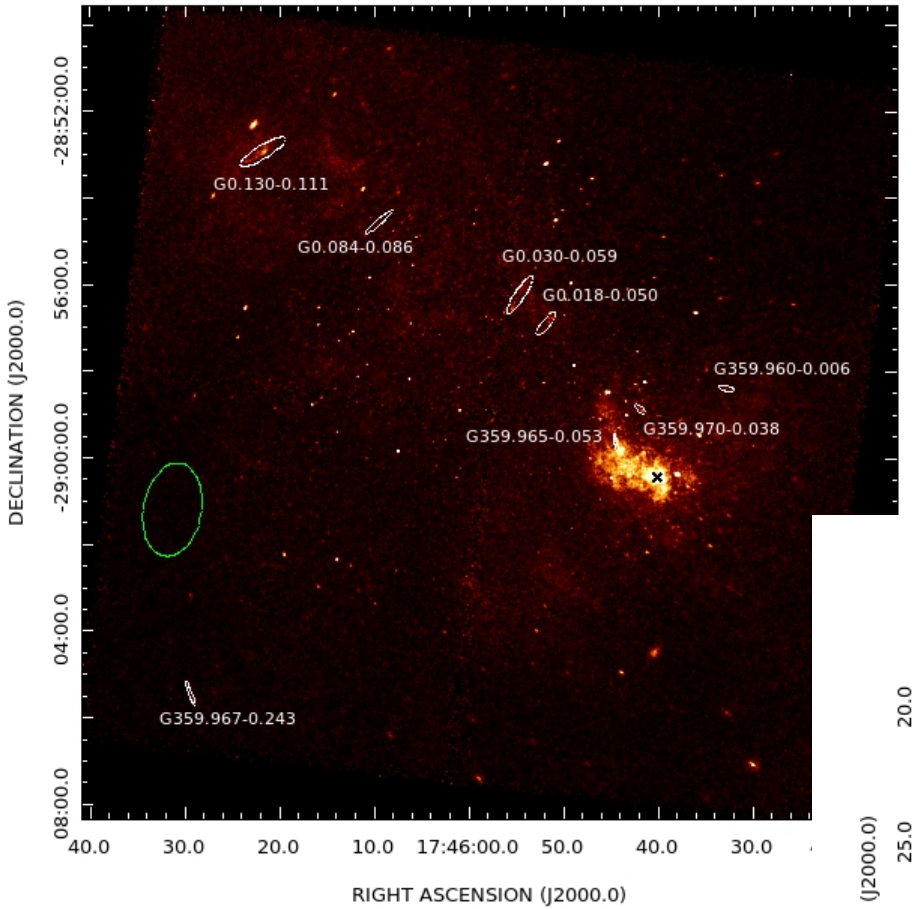

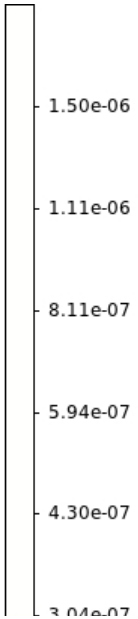

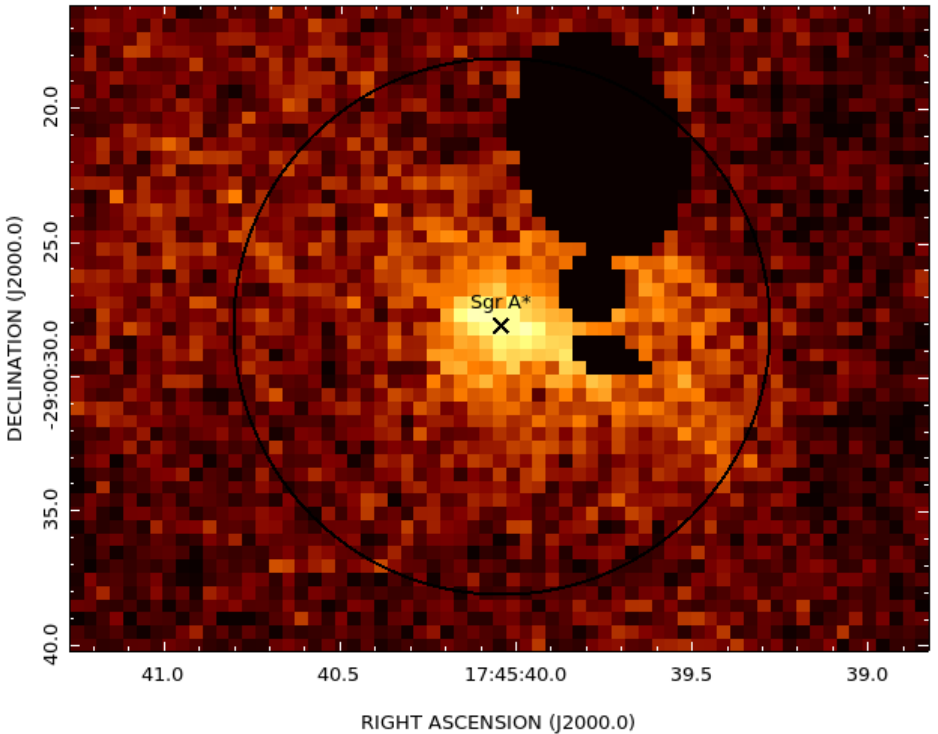

The Galactic Center:

Różańska + 2015

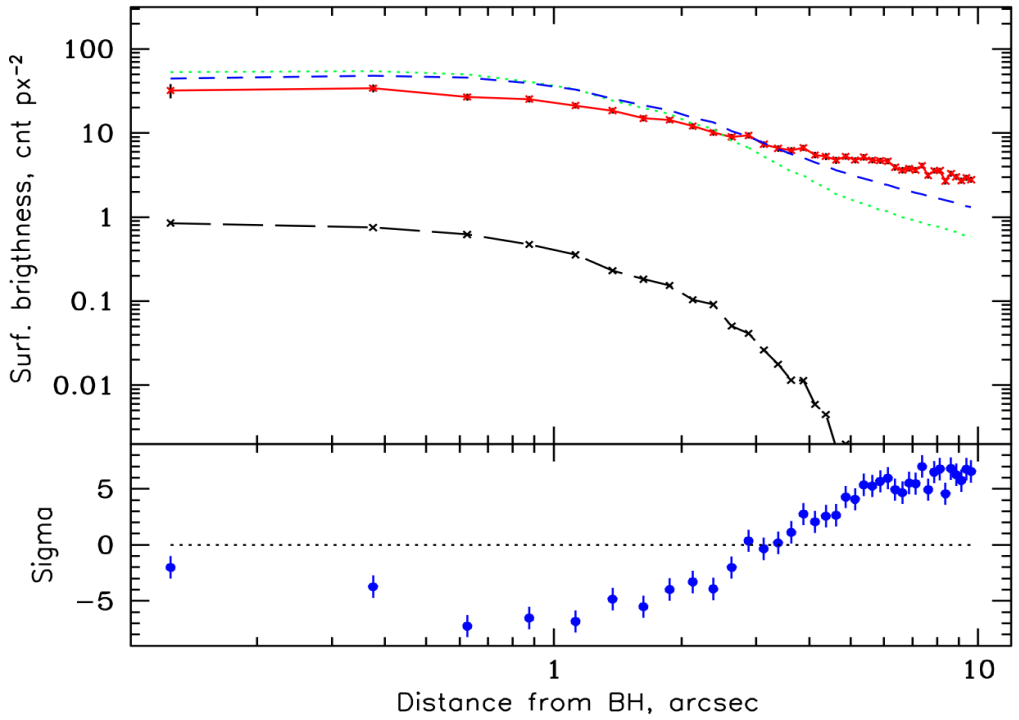

Fig. 3. Vicinity of the black hole up to 10″ from Sgr A*. Red points with errors represent the observed profile, and are connected by continuous line. The black long-dashed line is the normalized PSF. Two models convolved with PSF are also presented: green dotted line for T_e^{out} = 1 keV, and blue short-dashed line for T_e^{out} = 3.5 keV. Residuals are shown for the best fitted model in the range up to 10″, i.e. for T_e^{out} = 3.5 keV.

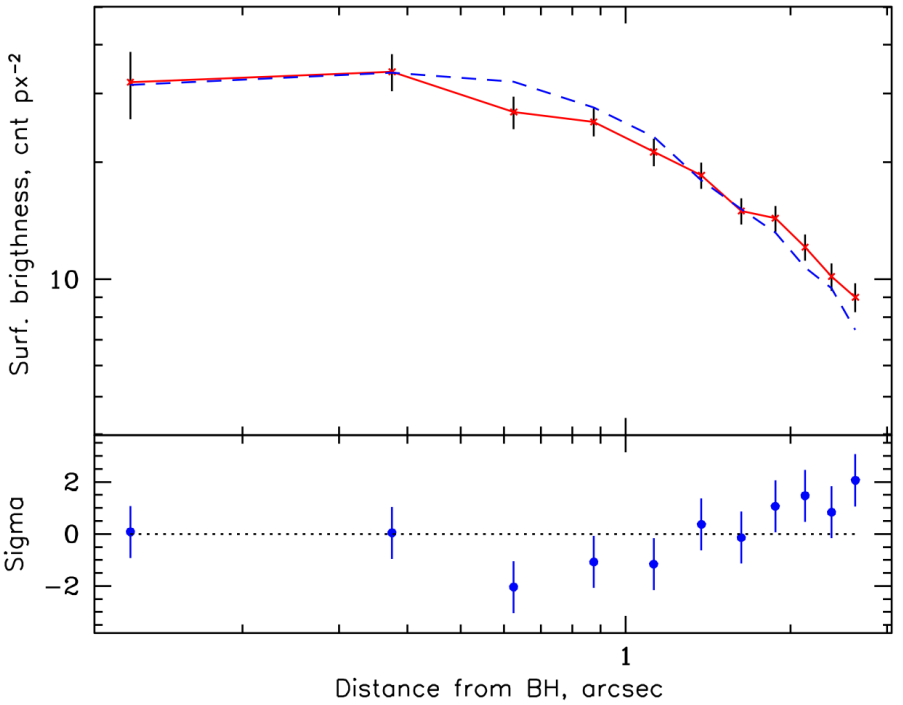

Fig. 6. Surface brightness profile up to 3″ from Sgr A*. Red points represent the observed profile, and are connected by a continuous line. The best fit model with T_e^{out} = 3.5 ± 0.3 keV and n_e^{out} = 18.3 ± 0.1 cm^{-3} is shown by a blue short-dashed line, and the fit residuals are presented in the *lower panel*.

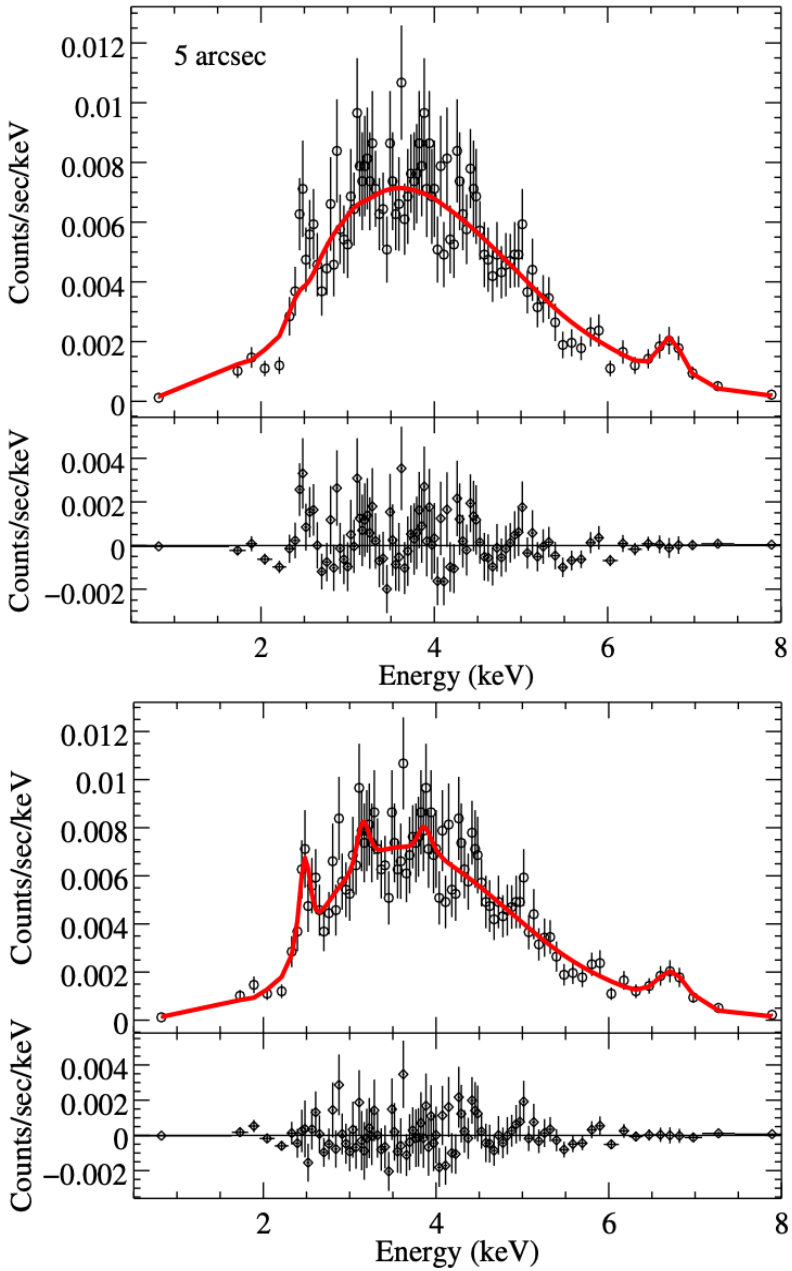

Fig. 4. Modelling of the spectrum extracted from the 5″ circular region around the Sgr A*. Both panels present fits with the distant background. The upper panel shows a model consisting of Galactic absorption (tbabs), thermal bremsstrahlung, and one Gaussian line to account for the iron emission. The lower panel shows a model with three additional Gaussian lines for the S, Ar, and Ca emission.

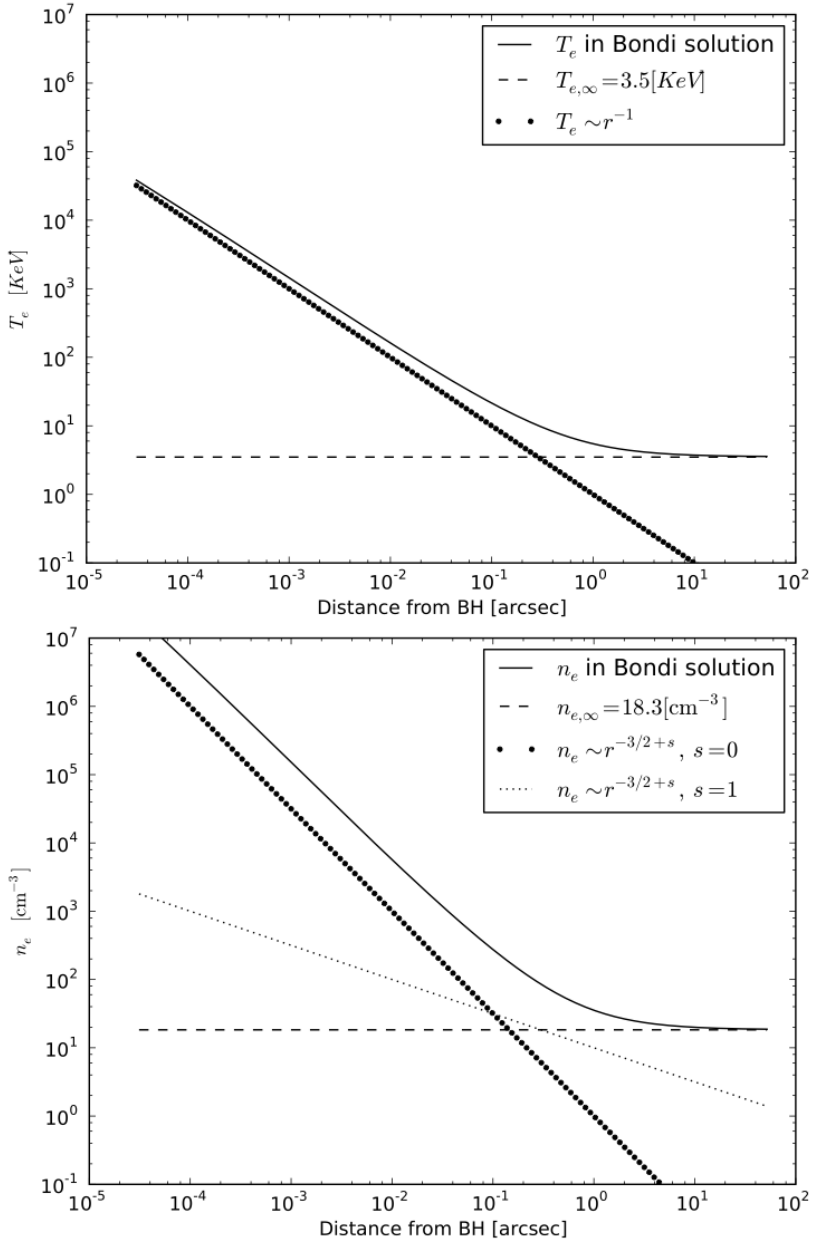

Fig. 7. Temperature and density profiles around Sgr A* for our best fitted model $T_e^{out} = 3.5 \pm 0.3$ keV and $n_e^{out} = 18.3 \pm 0.1$ cm^{-3}, *upper and lower panel*, respectively. The asymptotic values of T_e^{out} and n_e^{out} are marked as dashed lines. Additionally, we show the radial dependencies of the temperature and density in the RIAF model without ($s = 0$) and with ($s = 1$) an outflow. The normalization of the RIAF model is arbitrary.

The Galactic Center:

$$\mathrm{RM} = 8.1\times10^{5} \int n_{\mathrm{e}} B \mathrm{d}l$$

$$\mathrm{RM}^{*}_{\mathrm{GC}} = 5.6 \pm 0.7 \times 10^{5}\ \mathrm{rad/m^2}$$ Marrone + 2007

$$\mathrm{RM}^{*}_{\mathrm{Pulsar}} = 6.696 \pm 0.004 \times 10^{4}\ \mathrm{rad/m^2}$$ Eatough + 2013

ρ_∞ [cm^{-3}]	T_∞ [keV]	$\dot{M}$ [$M_\odot$ yr^{-1}]	$c_{s,\infty}$ [cm s^{-1}]	$\mathrm{RM_{GC}}$ ($\beta = 1$) [rad/m^2]	$\mathrm{RM_{GC}}$ ($\beta = 10^7$) [rad/m^2]	$\mathrm{RM_{Pulsar}}$ ($\beta = 1$) [rad/m^2]	$\mathrm{RM_{Pulsar}}$ ($\beta = 100$) [rad/m^2]
18.3	3.5	1.3×10^{-6}	7.4×10^{7}	2.1×10^{9}	6.6×10^{5}	5.2×10^{4}	5.2×10^{3}
18.4	3.5	1.3×10^{-6}	7.4×10^{7}	2.1×10^{9}	6.6×10^{5}	5.3×10^{4}	5.3×10^{3}

The Galactic Center: Różańska + 2015,2018

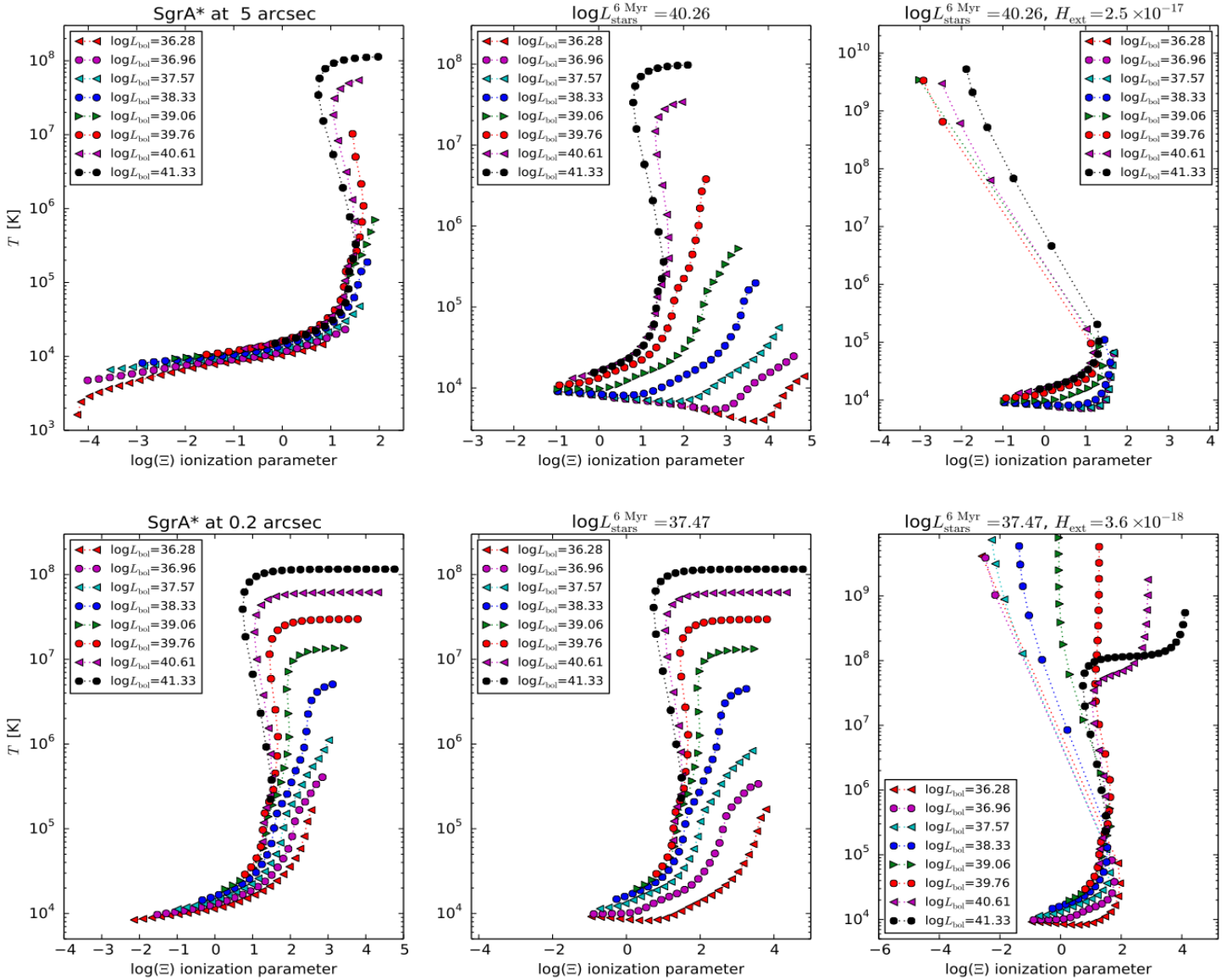

Figure 2. Solutions for S-curve of TI in the plane of temperature versus ionization parameter, as defined in equation (5), for different luminosity states of the radiation: from the central source only (left-hand panels), together with heating by stellar radiation (middle panels), and together with mechanical heating by winds (right-hand panels). Values of central source luminosity are marked within the panels. We present results for the gas located at 5 arcsec from Sgr A* (upper row of panels) and at 0.2 arcsec (bottom row of panels). The luminosity and volume mechanical heating are $\log(L_{\rm stars}/{\rm erg\ s^{-1}}) = 40.03$ and $H_{\rm ext} = 2.5 \times 10^{-17}$ erg s^{-1} cm^{-3}, respectively, at 5 arcsec and $\log(L_{\rm stars}/{\rm erg\ s^{-1}}) = 37.47$ and $H_{\rm ext} = 3.6 \times 10^{-18}$ erg s^{-1} cm^{-3}, respectively, at 0.2 arcsec from Sgr A*.

The Galactic Center: Różańska + 2015,2018

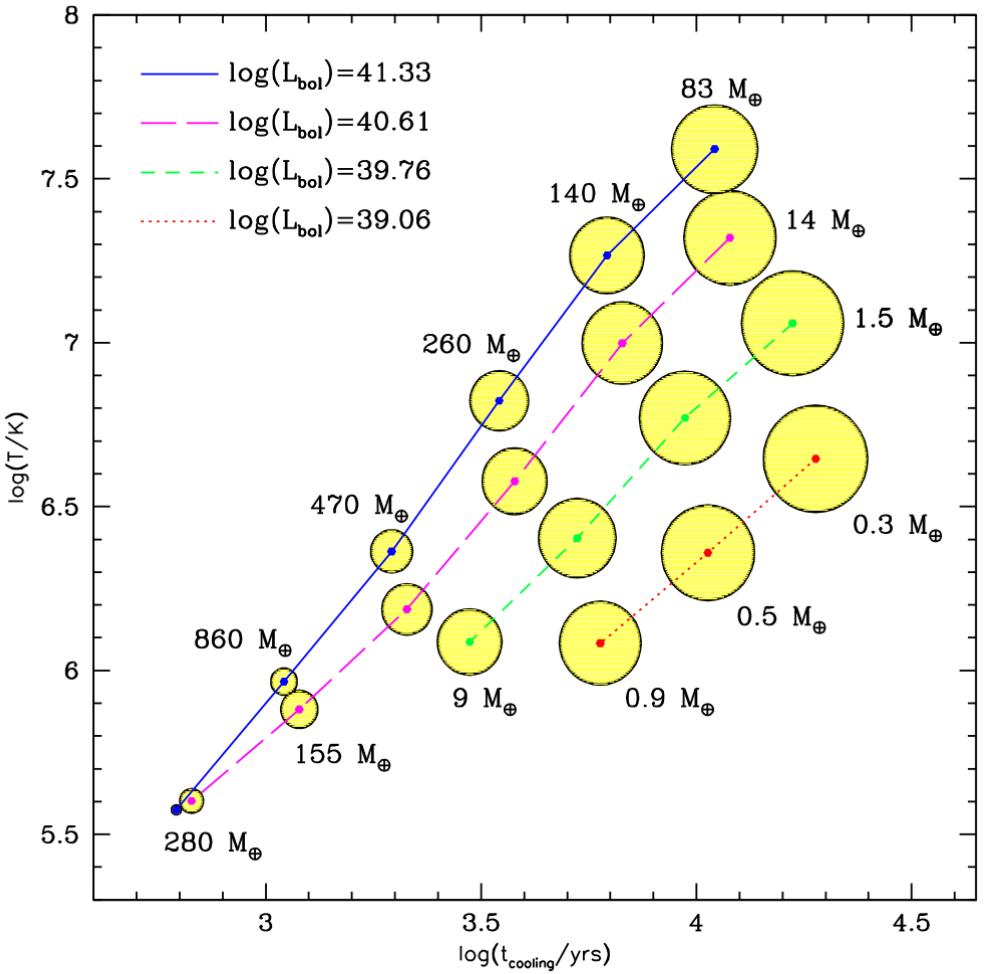

Figure 4. Size of clouds along an instability branch positioned in the log–log plot of cooling time $t_{\rm cooling}$ versus temperature T. Four different curves are plotted for different values of the bolometric luminosity, i.e. the four lines connect clouds that are produced by the same radiation field, as specified in the top-left corner of the plot. Along each curve, the radii of the yellow circles represent the Field length according to equation (3). Masses of clouds determined by equation (4) are given in units of Earth mass.

The Galactic Center: Różańska + 2015,2018

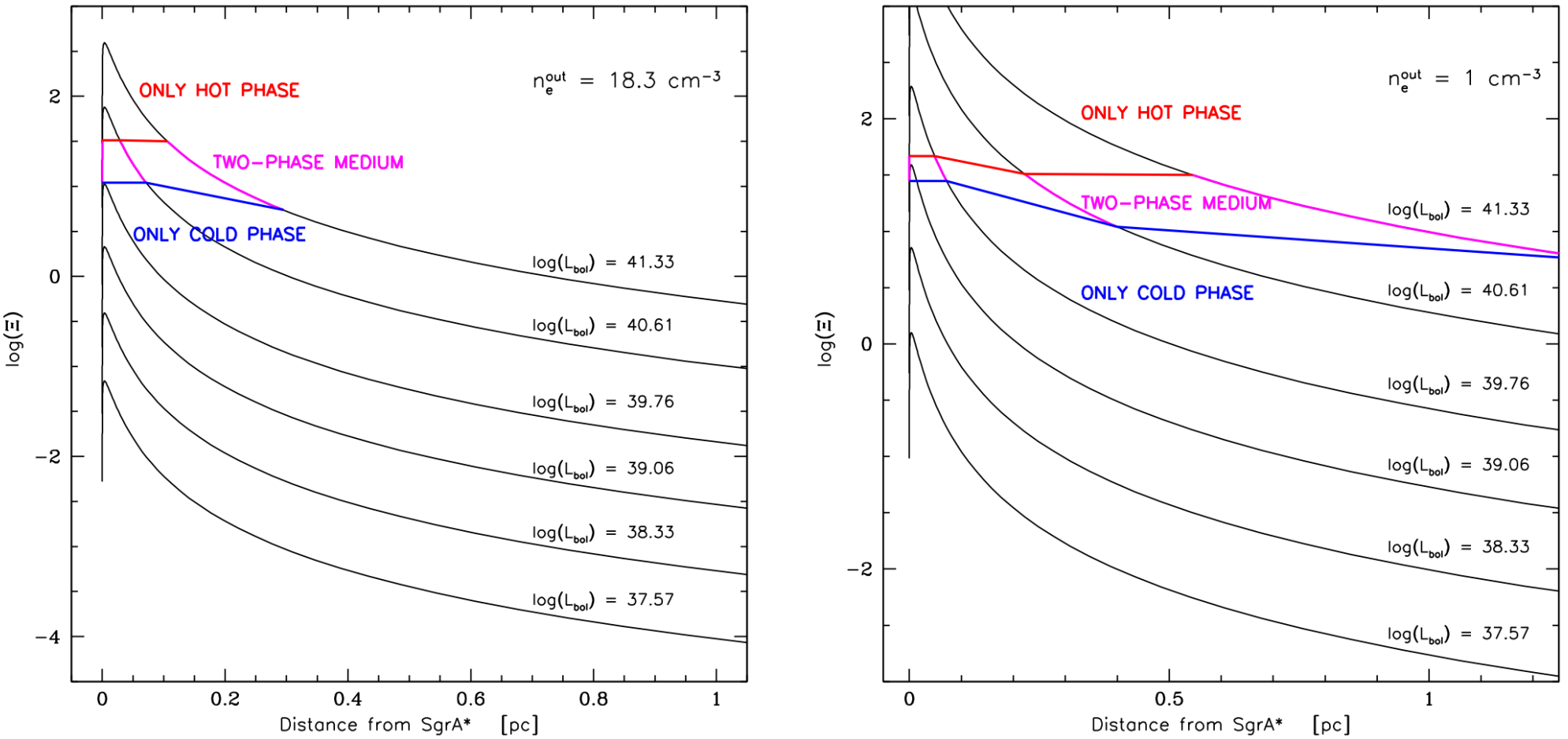

Figure 7. Instability strips for the different luminosity states for Bondi accretion flow on to Sgr A* for outer temperature $T_e^{out} = 3.5$ keV. The left panel shows cases for outer number density $n_e^{out} = 18.3$ cm^{-3} and the right panel for $n_e^{out} = 1$ cm^{-3}. The region between the coloured contours is for the two phase-medium, and its extent is shown by magenta lines for each luminosity state. The thermal instability can operate in the range of the high luminosity for Sgr A* that occurred in its past history.

Lecture on Feb. 14th – today's lecture

NEXT NEW LECTURE on Feb. 16th 2023

- You can still upload your HW#6 and hands-on results
  Up to the Feb. 19th (Copernicus birthday).

- theory, but we still practice

wi-fi password: a w sercu maj
We have eduroam as well